

## ABSTRACT

Title of Thesis: GROUNDTRUTH GENERATION AND DOCUMENT IMAGE DEGRADATION

Gang Zi, Master of Science, 2005

Thesis Directed By: Professor Rama Chellappa  
Department of Electrical and Computer Engineering  
University of Maryland at College Park

The problem of generating synthetic data for the training and evaluation of document analysis systems has been widely addressed in recent years. With the increased interest in processing multilingual sources, however, there is a tremendous need to be able to rapidly generate data in new languages and scripts, without the need to develop specialized systems. We have developed a system, which uses language support of the MS Windows operating system combined with custom print drivers to render tiff images simultaneously with windows Enhanced Metafile directives. The metafile information is parsed to generate zone, line, word, and character ground truth including location, font information and content in any language supported by Windows. The resulting images can be physically or synthetically degraded by our degradation modules, and used for training and evaluating Optical Character Recognition (OCR) systems. Our document image degradation methodology incorporates several often-encountered types of noise at the page and pixel levels. Examples of OCR evaluation and synthetically degraded document images are given to demonstrate the effectiveness.

GROUNDTRUTH GENERATION AND DOCUMENT IMAGE DEGRADATION

By Gang Zi

Thesis submitted to the Faculty of the Graduate School of the  
University of Maryland, College Park, in partial fulfillment  
of the requirements for the degree of  
Master of Science  
2005

Advisory Committee:

Professor Rama Chellappa, Chair  
Dr. David Doermann  
Professor Ramani Duraiswami

© Copyright by  
Gang Zi  
2005

## Acknowledgements

I would like to express sincere thanks to Dr. David Doermann and Prof. Rama Chellappa, for their continuous support, guidance, and help throughout my study. Dr. Doermann's vision of document analysis has been a constant source of inspiration, and greatly benefits this project. I would also like to express my gratitude to Prof. Ramani Duraiswami for being on the committee, and reviewing the thesis.

Also, I want to thank all the faculty and staff in Language and Media Processing Lab (LAMP), especially to Ms. Denise Best, and the Department of Electrical and Computer Engineering for giving me every assistance to fulfill the requirements. The list won't be complete without thanking colleagues in LAMP, especially to Jian Liang, Yefeng Zheng, Huanfeng Ma, and Yi Li, for stimulating discussions.

Last but not least I wish to express my gratitude to my wife Ling for her love, support, and encouragement.

# Table of Contents

Acknowledgements.....	ii
Table of Contents.....	iii
List of Tables.....	iv
List of Figures.....	v
Chapter 1 Introduction.....	1
1.1 Scope of thesis.....	3
1.2 Organization of thesis.....	4
Chapter 2 Literature review.....	6
2.1 Synthetic data sets and ground truth generation.....	6
2.2 Document image degradation models.....	10
2.3 OCR evaluation.....	12
Chapter 3 Multi-lingual OCR evaluation.....	14
3.1 System overview.....	14
3.2 Ground truth generator.....	16
3.2.1 Obtaining ground truth files from the enhanced meta files.....	19
3.2.2 Font mapping files and parser tools.....	21
3.3 Evaluation tools.....	27
3.4 Evaluation examples.....	28
Chapter 4 Ground truth alignment.....	33
4.1 Alignment overview.....	33
4.2 Alignment experiments.....	36
Chapter 5 Document image degradation.....	39
5.1 Image degradation architecture:.....	39
5.2 Page level noise.....	40
5.3 Pixel level noise.....	45
5.4 Bleed-through and show-through noise.....	49
5.4.1 Background.....	49
5.4.2. Approach.....	50
5.4.3 Experiments.....	53
5.5 Implementation.....	56
Chapter 6 Summary.....	58
6.1 Summary of contributions.....	58
Reference.....	60

## List of Tables

TABLE 1 EXAMPLE OF SAME CHARACTER IN DIFFERENT FONTS .....	22
TABLE 2 OCR PERFORMANCE FOR SYNTHETIC IMAGES.....	31
TABLE 3 OCR PERFORMANCE FOR SCANNED IMAGES WITH DIFFERENT RESOLUTIONS	32
TABLE 4 FUNCTION AND PARAMETER LIST FOR DOCUMENT DEGRADATION CLASS .....	57

# List of Figures

FIGURE 3. 1 OCR EVALUATION SYSTEM ARCHITECTURE .....	15
FIGURE 3. 2 EXAMPLES OF OVERLAID IMAGES. (A) CHINESE DOCUMENT IMAGE AT THE CHARACTER LEVEL; (B) ENGLISH DOCUMENT IMAGE AT THE WORD LEVEL; (C) JAPANESE DOCUMENT IMAGE AT THE LINE LEVEL; (D) ARABIC DOCUMENT IMAGE AT THE ZONE LEVEL .....	16
FIGURE 3. 3 CORE GROUND TRUTH FILE EXAMPLE .....	17
FIGURE 3. 4 HTML GROUND TRUTH FILE EXAMPLE FOR THAI.....	18
FIGURE 3. 5 EMF FILE EXAMPLE .....	20
FIGURE 3. 6 COMPOSITION OF ONE CHARACTER FROM SEVERAL GLYPH INDICES .....	22
FIGURE 3. 7 ARABIC CHARACTER “HA” IN ISOLATED, INITIAL, MIDDLE, AND FINAL FORM.....	23
FIGURE 3. 8 EXAMPLE OF A DUMPED FONT FILE.....	24
FIGURE 3. 9 EXAMPLE OF FONT VERIFICATION FILE FOR MANGAL FONT.....	26
FIGURE 3. 10 EXAMPLE OF FONT MAPPING FILE FOR MANGAL FONT.....	26
FIGURE 3. 11 SCREEN SHOT OF EVALUATION SYSTEM INTERFACE .....	28
FIGURE 3. 12 ACCURACY SCATTER PLOT FOR TWO OCR WITH SYNTHETIC IMAGES.....	30
FIGURE 3. 13 OVERALL PERFORMANCES DIAGRAM FOR TWO OCR WITH SCANNED IMAGES .....	30
FIGURE 3. 14 SORTED ACCURACY RATE IN DIFFERENT RUNS .....	31
FIGURE 3. 15 ACCURACY SCATTER PLOT FOR ONE OCR WITH TWO NOISE LEVEL IMAGES .....	32
FIGURE 4. 1 NOISE FREE IMAGE AND DEGRADED IMAGE ALIGNMENT PROCEDURE .....	34
FIGURE 4. 2 NOISE FREE IMAGE AND FAXED IMAGE EXAMPLE .....	35
FIGURE 4. 3 EXAMPLE OF SKEW AND SHRINK/ENLARGE DOCUMENT EXAMPLE .....	36
FIGURE 4. 4 EXAMPLE OF ALIGNED ENGLISH DOCUMENT .....	37

FIGURE 4. 5 EXAMPLE OF ALIGNED CHINESE DOCUMENT .....	37
FIGURE 4. 6 DOCUMENT IMAGE WITH COMPLEX CONTENT FROM CAMERA .....	38
FIGURE 4. 7 EXAMPLE OF ALIGNED CAMERA IMAGE.....	38
FIGURE 5. 1 IMAGE DEGRADATION AND APPLICATION ARCHITECTURE .....	39
FIGURE 5. 2 EXAMPLE OF ROTATION OF 45° AND ROTATION OF 10° .....	41
FIGURE 5. 3 2D GAUSSIAN FUNCTION AND SAMPLING GRID .....	42
FIGURE 5. 4 EXAMPLE OF A DOCUMENT BEFORE AND AFTER BLURRING .....	43
FIGURE 5. 5 EXAMPLE OF SCATTERING LINES ON DOCUMENT IMAGE.....	44
FIGURE 5. 6 EXAMPLE OF MERGE (A) NOISE FREE IMAGE (B) NOISE TEMPLATE (C) DEGRADED IMAGE .....	45
FIGURE 5. 7 EXAMPLE OF SPECKLES AND JITTER (A) DEGRADED IMAGE (B) JITTER EFFECT (C) SPECKLES .....	47
FIGURE 5. 8 THE EFFECT OF PIXEL LEVEL DEGRADATION. (A) ORIGINAL IMAGE; (B) DEGRADED IN LOW NOISE LEVEL; (C) DEGRADED IN HIGH NOISE LEVEL. ....	48
FIGURE 5. 9 THE SHOW-THROUGH EFFECT OF A SCANNED NEWSPAPER.....	49
FIGURE 5. 10 EXAMPLE OF BINARY FRONT SIDE IMAGE .....	51
FIGURE 5. 11 (A) FRONT SIDE IMAGE; (B) BACK SIDE IMAGE FROM FIGURE 5.9.....	54
FIGURE 5. 12 (A) SYNTHETIC SCAN-THROUGH IMAGE WITH $\alpha = 0.1$ , AND THRESHOLD = 60 (B) REAL SCANNED NEWSPAPER .....	56

## Chapter 1 Introduction

During the past several decades, document image analysis and Optical Character Recognition (OCR) have been widely successful. Many desktop solutions continue to appear and work well for high quality input. Although many commercial OCR products have merged in the market, this consolidation is helping customers with more complete document image conversion, storage and retrieval solutions. With help from advanced image processing methods and pattern recognition techniques, some of the OCR vendors claim a near 100% accuracy rate on typical office documents. However, there are still some open problems, such as improving OCR accuracy on poor quality images from devices such as fax, dot matrix and impact printers, and photocopiers, or from physically degraded documents. Furthermore, complex layouts, multiple-languages and combined content, such as handwriting annotations, provide additional challenges.

In this thesis, we are focusing on how to generate representative training data and how to evaluate systems in support of these open problems. It is well known that the accuracy of a recognition system depends not only on the features and classifiers, but also on the size and quality of training sets. Obtaining a significant corpus of document images and symbolic ground truth is an important precursor for training and evaluating document analysis systems. Often, documents are scanned page by page, ground truth text is keyed character by character, and bounding boxes are drawn manually. This process is labor-intensive and error prone, and becomes increasingly difficult when processing multi-lingual collections with thousands of pages. Native

speakers and a special input environment are required for non-Latin ground truth generation, and such tools may not be widely available.

To bypass manual keying in symbolic data, researchers have typically used existing ground truth data sets. One widely adopted source data set is the University of Washington (UW) data set. The first release has two thousand English and Japanese technical document images, and has been widely used by OCR developers. However, if the researchers want to develop or test their recognition system on other document styles or in other languages, those data sets cannot provide much help. Some researchers have used the Bible because it has an additional advantage of appearing in multiple languages so that it can serve as a source of parallel text. It is not convenient, however, if the users need to test the OCR systems on their own documents, which may have specific vocabulary.

A method using Device Independent (DVI) files and LATEX typesetting has been proposed to address this problem [5] by providing a way to generate images from electronic text. The text is keyed in LATEX environment manually, and is compiled to generate DVI files. Those DVI files are transformed to TIFF images using DVI2TIFF. Although this method provides a convenient way to create accurate ground truth files, the manual formatting is still error prone, and may result in significant cost for multilingual documents. Furthermore, a native speaker is still needed to key in the characters if we would like to process non-Latin languages.

The second issue we are interested in is how to evaluate OCR in an unbiased way. Because the OCR systems are evaluated on different data sets, a 99% accuracy level of one OCR system is different from a 99% accuracy level of another OCR

system. Furthermore, those accuracy rates are suspect when the data sets used in evaluation are not representative of the intended document population.

As mentioned above, the prohibitive expense of manually generated ground truth, and the prior bias introduced by using those existing data sets have prompted us to use synthetic data as a complement to real data. The problem of generating synthetic data for the training and evaluation of document analysis systems has been widely addressed in recent years.

In this thesis, we will describe a multilingual OCR evaluation system, which includes a document formatter, a ground truth generator (GTG), an integrated evaluation tool, and a document image degradation tool. This system provides a universal framework to generate training and evaluation data sets on a large scale. Beginning with electronic text, our ground truth generator produces noise-free images and ground truth files. Since the text can be effortlessly copied from the Internet or existing electronic sources instead of being manually keyed in, this method is extremely helpful when dealing with new languages and new scripts. In most cases, a person who wants to create the data sets can do so without being a native speaker of that language.

## 1.1 Scope of thesis

In this thesis, we address some aspects of the document analysis system's training and evaluation, and document image degradation, with a focus on ground truth generation and degradation.

The complete textual ground truth for a document image includes symbolic text files, font, character size, and position information for each symbol, as well as the

location of regions containing graphics, logos etc. In our evaluation system, noise free images and the physically or synthetically degraded images are fed to underlying OCR systems to generate recognized text. A set of document image degradation methods have been proposed and implemented to generate synthetic degradations, including page level and pixel level noise.

The following summarizes the key contributions of this thesis:

- An automatic multilingual OCR evaluation system has been proposed, and implemented. This system includes document formatter, ground truth generator, font parser and verifier, and evaluation sub-systems.
- A method to align the ground truth files with degraded images has been proposed and implemented. This method uses linear transformation to model the print-copy-fax-scan procedure.
- A document degradation methodology has been proposed and implemented. Methods include blur, speckle, rotation, jitter, resolution change, pixel drift, horizontal and vertical lines, and page show-through.

## 1.2 Organization of thesis

This thesis is organized into six chapters. In Chapter 2 we survey related work in the areas of ground truth generation, OCR evaluation, and document image degradation. We present our multi-lingual OCR evaluation system in Chapter 3, where the system architecture, the Extended Meta File (EMF) structure, our font parser tools used to create and verify the font mapping files, and the evaluation tools are explained. Two Chinese OCR systems are evaluated to illustrate the system. In Chapter 4, a method to align noise free ground truth with degraded images is

proposed; and experiments of faxed and camera captured images show the effectiveness of this transformation. A document image degradation methodology is proposed in Chapter 5, where page level and pixel level degradation methods are explained in detail. Chapter 6 contains a summary of the accomplishments.

## Chapter 2 Literature review

We focus our literature review in the areas of using synthetic data sets, generating ground truth, degrading document images, and OCR evaluation.

### 2.1 Synthetic data sets and ground truth generation

Using synthetic data, which is “born digital” and/or synthetically degraded, has many advantages over scanning and manual entry, including rapid generation of datasets at lower cost, continuous control of degradation level, and convenient testing of the same underlying document content with different corruption methods [1]. Although many have argued that synthetic data sets do not provide a representative corpus, if used correctly, it can provide a valuable complement to expensive hand created datasets. Our experiments show that there is often no significant difference between synthetically generated data and the physically generated in terms of OCR performance. For instance, OCR achieves 96.67% accuracy rate on synthetic data, while 96.25% on the same physically scanned document data on 300 dpi. Inspired by the method described in [2] to validate the defect model, we can safely conjecture that the synthetic data is validated if the OCR errors obtained are indistinguishable from the errors obtained when using real scanned data. In general this has proven to be an elusive goal so we will provide no quantitative validation. To validate the local degradation models, the author in [5] proposed a statistic methodology based on a nonparametric, two-sample permutation test, and used a power function to choose algorithm variables.

The impact of image quality and the representativeness of training image data sets on OCR performance were originally addressed by Baird in [3]. He claims accuracy of a recognition system depends not only on the features and classifiers, but also on the size and the quality of training sets. Using synthetic data in an appropriate way may help determine the weaknesses of the underlying OCR and document analysis systems.

Typically, the ground truth data sets are created manually. Documents are scanned page by page, ground truth text is keyed in character by character, and bounding boxes are drawn on the images manually. Because a large quantity of ground truth data is required in order to give an accurate measurement of the performance of document analysis and recognition systems, researchers have created some data sets for training and evaluation, such as the University of Washington Document Image Database [4]. This data set has thousands of English technical document images, and corresponding ground truth files, including zone and page bounding boxes, attributes, and ASCII text for each constituent document. It provides a valuable platform to develop and evaluate underlying systems. However, this data set is not helpful if the target documents are in other languages, other document styles, or have different quality levels. In those situations, the researchers have to create their own ground truth data sets.

To obtain ground truth datasets at minimum cost, automated ground truth generation methods have been proposed. In [5], the author presents an approach to obtain ground truth files. First, the document characters are formatted in LATEX, either by manual transcription or by reformatting e-text. The typesetting files are then

compiled to device independent (DVI) files. Ground truth can be extracted from those typesetting files; while the noise free document images can be obtained by using DVI2TIFF. The requirement of DVI files and LATEX typesetting, however, limits the practical application in many cases, as LATEX does not support all languages. Furthermore, the manual entry is still error-prone and may be prohibitively expensive when processing multi-lingual documents with thousands of pages.

To overcome the inconvenience of keying in symbolic data, researchers have also used sources in which both hard copy and electronic form already exist. The use of the Bible is proposed in [6] because the electronic symbolic ground truth exists in many of the world's languages, and thus can serve as a source of parallel text. In [6], groundtruth files in Arabic, English, and French Bibles were collected, converted into DVI files from ASCII text using LATEX typesetting, and TIFF images were obtained from those DVI files. The Arabic Bible was also physically scanned. This data set provides a broader platform for multi-lingual OCR training and evaluation, but it is not expandable. Users may want to test the OCR systems in a specific domain, which contains many modern words not included in the Bible.

When groundtruth is generated, there are a variety of options for representation. A complete groundtruth file should include the information of coordinates of each character, word, line, and zone when possible. The higher-level information is critical for tasks, such as document segmentation and layout analysis. After obtaining ground truth for ideal images, degraded versions are typically obtained by copying, faxing, and/or rescanning, but realigning the ground truth can be

a challenge. In [8], the author aligns the ground truth from ideal images with the scanned images using a linear transformation matrix. The four outermost points, which are measured from the four corners of all the bounding boxes of connected components, are located on both the noise free image and the corresponding degraded image. The coordinates of the four feature point pairs are used to calculate the projective transformation. Then the bounding boxes of the ideal image are mapped to the degraded image using the computed transformation matrix. A local adjustment is employed to compensate for nonlinear factors in print-scan procedure. Because they are using the four outermost bounding box corners as feature points, the procedure is vulnerable in noisy images so that many more points are used to attack this problem in [9].

Several ground truthing tools have been developed in order to reduce the labor of creating data sets. Groundskeeper [10] is a tool to create and edit document segmentation ground-truth. This tool allows a user to display a document image, draw zones of various types around different page regions, and label each zone with attributes such as type, sub-type, parent zone, and attached zones *etc.* TrueViz [11] is a java program to visualize and edit ground truth or metadata files. This tool provides text editing, display, search functions based on Unicode for the image and metadata. The results are saved in XML format.

Synthetic data sets have been widely used recently. In [12], synthetic data is generated and used for training a Hidden Markov Model (HMM) based Arabic OCR system. Symbolic ground truth is keyed in and formatted in a LATEX environment,

while the noise free images are obtained from the DVI files. The procedure requires a native speaker, and a specific input environment to key in the non-Latin documents.

Additional synthetic training data is utilized in [13] to improve the performance of a HMM based handwriting recognition system. A perturbation model, which is based on the summation of a number of CosineWave functions, has been used to get synthetic text lines from existing real handwritten lines. Substantial improvement was observed.

In [14], a line drawing degradation model was proposed for the purpose of evaluating line detection algorithms using synthetic data. This model simulates some types of noise, such as Gaussian noise, blur, hard pencil noise and motion noise, introduced during the production, and photocopying of technical documents. The authors use “Black Box Testing” method to validate the model. They compare the difference between the real documents and the synthetically generated documents with noise levels estimated from real images. If the difference is smaller than the threshold, this model will be accepted. However, higher order statistic analysis is needed for their validation method.

The work mentioned above suggests that if used correctly, the synthetic data can provide a valuable complement to expensive manually created datasets, in practical situations.

## 2.2 Document image degradation models

The study of explicit, quantitative and parameterized models of defects became a focal point with the work of Baird in [3], [15], [16]. Baird proposed in his pioneering work, a parameterized model to approximate some aspects of the physics

of machine printing and imaging of text, such as affine transform, threshold, and speckle. This model accounts primarily for per-symbol and per-pixel defects. The author also applied bootstrapping and power function analysis to this physics-based model in [16]. Using this model and the synthetically generated character images, the authors in [17] studied a binary tree classifier's accuracy as a function of several important model parameters. Those parameters include blur, binarization threshold, and the variance of pixel sensor sensitivity. They found that two defects (blur and threshold) affect the classification significantly, continuously, and monotonically.

As pointed out in [5], this model mainly advocates the use of isolated degraded characters, and does not reflect some important aspects, such as touching characters and occurrence probabilities. The authors then extended their work and proposed a document degradation model (DDM) [18], which is based on a local morphological model, to randomly invert pixels and blur them during the degradation procedure. The inverting probability is controlled by the decaying speed of an exponential function, but accounts for only the local statistical characteristics.

Both models are used widely in document analysis and recognition systems. For example, to study the effect of degraded images on a font recognition system in [19], three artificially generated images are used to evaluate the system. To allow the fonts recognition from degraded images without any specific training, two transformation approaches are used: font model transformation, and feature values transformation. Baird's model was used in [20] to create large-scale degraded image data sets for document image decoding system training and evaluation. Their work shows high accuracy from trained models on even severely degraded images, and

significant improvement compared to untrained models. Furthermore, no manual segmentation is needed in creating the training data set. Unfortunately, neither of these models claims to handle “clutter” noise that may be present in real documents.

In [21], the author proposed a method to create a large number of groundtruthed real images from the existing data set with a fraction of the cost. The images in an existing data set are printed out, physically degraded, and then re-scanned. The degradation procedure includes copying, smearing, adding coffee and ink stains etc. After re-scanning, bounding boxes are drawn manually on those degraded images. The author claims that creating the page and zone box files only cost 1% in the whole ground truthing procedure. Although this method can bootstrap existing data sets, it cannot create new data sets. On the other hand, errors and noise can be introduced in the manual degradation procedure as well.

A two state Markov chain model is proposed in [22]. This method depicts the document degradation with two states: a random state to model salt and pepper noise, and a burst state to model blurring over a large document region. The power function in [5] is used in this paper to validate their model. To estimate the transition probabilities of their model, a genetic algorithm is suggested in their paper.

### 2.3 OCR evaluation

Characterizing a profile of OCR systems provides useful information [23], such as predicting OCR performance in a larger system, monitoring progress etc. It is also very helpful to find vulnerable parts of the document recognition system under some circumstances. Thus a valuable feedback can be obtained through the OCR evaluation.

As described in [24], there are two types of OCR evaluation: black box evaluation and white box evaluation. The black box evaluation treats the OCR system as an indivisible unit, while the white box evaluation will characterize the performance of each sub modules of document recognition system, such as preprocessing, segmentation, and classification modules. The white box evaluation is only applicable if the researcher can access the intermediate output of the OCR software.

In the following chapters, we present a methodology to evaluate multi-lingual OCR systems. Our method includes a ground truth generator to create complete ground truth files and noise free images automatically, and a tool to create synthetically degraded images, with both the page level and pixel level noise.

## Chapter 3 Multi-lingual OCR evaluation

In many situations, it is useful to measure the effect of underlying OCR software in a cascading system with down stream processes, such as Information Retrieval (IR) and Machine Translation (MT) system. As we mentioned before, using existing data sets can be biased; while manually ground truthing can be prohibitively expensive, and become extremely difficult when processing multi-lingual collections with thousands of pages.

In this chapter, we present a methodology to generate noise free document images and symbolic groundtruth files automatically using a custom print driver and meta-file information. The system architecture is introduced and briefly discussed in Section 3.1. The main component of our system, the groundtruth generator is explained in detail in Section 3.2. This section also depicts the structure of Enhanced Meta-File (EMF) and our font parser, which is used to extract font-mapping files from TrueType Font (TTF) files. In Section 3.3, we describe the evaluation tools. We evaluate two major Chinese OCR software packages in Section 3.4.

### 3.1 System overview

The architecture of our evaluation system is shown in Figure 3.1.

Beginning with electronic text in a standard encoding, documents are either manually structured and formatted or passed through an XML formatter to obtain a structured document instance. From the structured documents, we generate noise-free images and ground truth files by using custom print driver and metafile information via a parser/renderer. The system relies on the Microsoft windows operation

system's use of enhanced metafile directives to provide a unified representation that includes Unicode glyph information and the physical location of each character on the page.

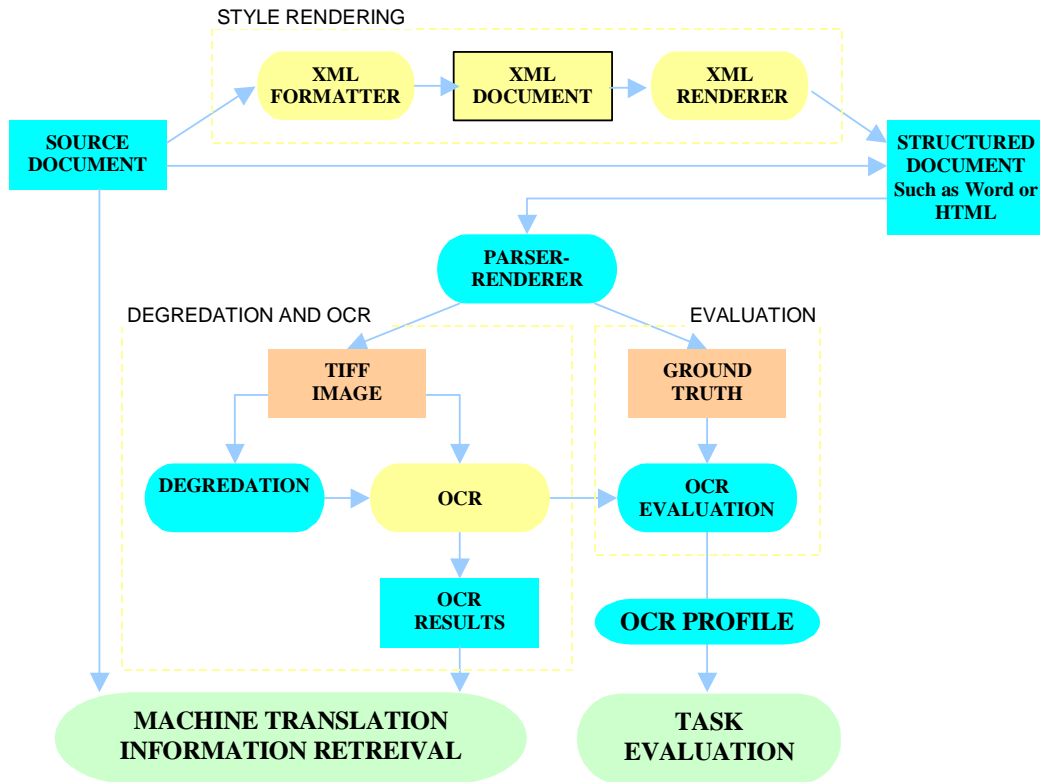


Figure 3. 1 OCR evaluation system architecture

Degraded images can then be obtained physically by printing, scanning and faxing, or be obtained synthetically by using degradation methods (Chapter 5). Finally, those ideal and degraded images are passed through an OCR system for evaluation. The results can also be used to measure the effect of OCR on down stream processes, such as information retrieval (IR), and machine translation (MT).

Our method is especially helpful in generating non-Latin ground truth. The user can copy and paste the document in the target language from the website, then create data sets using our system.

### 3.2 Ground truth generator

In our system, the ground truth generator (GTG) is used to obtain the synthetic noise free images, and parse the symbolic ground truth files from EMF files.

First, the structured documents are fed to GTG system. Image files at different resolutions and the metafiles are obtained via a custom printer driver. From the metafiles, we obtain character codes, font and layout information, for each symbol rendered. Because the ground truth files are parsed from metafiles, which rely only on the font files installed on the computer, the Unicode and original coding groundtruth files can be obtained accurately and rapidly. We've tested our system on dozens of languages, including Arabic, Chinese, Farsi, Hindi, Japanese, Korean, Thai, and Pashto, and our system provides a universal framework to generate groundtruth files for multi lingual documents.

For debugging purpose, images and layout information are used to create overlaid images, where the bounding boxes are displayed at the character, word, line, and zone levels. Examples in different zoning levels are given in Figure 3.2.

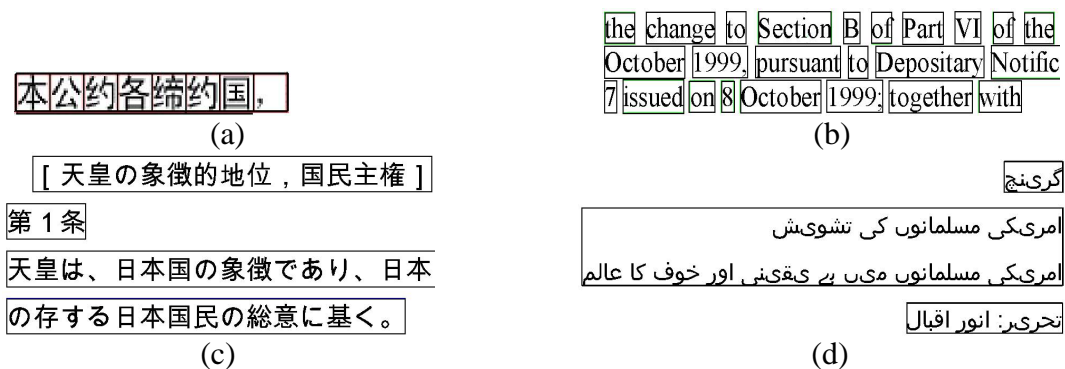


Figure 3. 2 Examples of overlaid images. (a) Chinese document image at the character level; (b) English document image at the word level; (c) Japanese document image at the line level; (d) Arabic document image at the zone level

Three kinds of ground truth files are generated by GTG: core ground truth files, raw ground truth files, and structured ground truth files.

- Core ground truth files contain the position information at each symbol, line, zone level and the identity of each symbol (Figure 3.3).
- Raw files are in Unicode format or in original coding format. These files can be used to compare with OCR results in evaluation. As in Chinese OCR evaluation, if the OCR output is in GB2312, then the raw ground truth files in original encoding should be used in comparison.
- Structured ground truth files include HTML files and XML files. As a debugging tool, the HTML files can be used to check whether the ground truth file is the same with the original text (Figure 3.4). The XML files are used for data exchange or storage (Figure 3.5).

```

CONTENT (pixels): (584,591,1940,2638)
PAGE SIZE (mm): (0,0,213,273)
RESOLUTION: 301 dpi
Font 0: Arial Unicode MS, HANGUL_CHARSET, 7
Font 1: Arial Unicode MS, SHIFTJIS_CHARSET, 7
ZONE 0: ( 584, 591, 1817, 634) T
LINE 0: ( 584, 591, 1817, 634)
WORD 0: ( 584, 591, 683, 634) 0
CHAR 0: ( 584, 591, 617, 634), 46021, 1 0xB3C5 (46021)
CHAR 1: ( 617, 591, 650, 634), 51068, 1 0xC77C (51068)
CHAR 2: ( 650, 591, 683, 634), 51032, 1 0xC758 (51032)
CHAR 3: ( 683, 591, 692, 634), 32, 1 0x0020 (32)
WORD 1: ( 692, 591, 792, 634) 0
CHAR 0: ( 693, 591, 726, 634), 51088, 1 0xC790 (51088)
CHAR 1: ( 726, 591, 759, 634), 46041, 1 0xB3D9 (46041)
CHAR 2: ( 759, 591, 792, 634), 52264, 1 0xCC28 (52264)
CHAR 3: ( 792, 591, 801, 634), 32, 1 0x0020 (32)
WORD 2: ( 801, 591, 935, 634) 0
CHAR 0: ( 802, 591, 835, 634), 47700, 1 0xBA54 (47700)
CHAR 1: ( 835, 591, 868, 634), 51060, 1 0xC774 (51060)
CHAR 2: ( 868, 591, 902, 634), 52964, 1 0xC EE4 (52964)
CHAR 3: ( 902, 591, 935, 634), 51064, 1 0xC778 (51064)
CHAR 4: ( 935, 591, 944, 634), 32, 1 0x0020 (32)
WORD 3: ( 944, 591, 1026, 634) 1
CHAR 0: ( 944, 591, 967, 634), 66, 1 0x0042 (66)
CHAR 1: ( 967, 591, 995, 634), 77, 1 0x004D (77)
CHAR 2: ( 995, 591, 1026, 634), 87, 1 0x0057 (87)
CHAR 3: (1026, 591, 1035, 634), 32, 1 0x0020 (32)
WORD 4: (1035, 591, 1135, 634) 0
CHAR 0: (1035, 591, 1068, 634), 54764, 1 0xD5EC (54764)
CHAR 1: (1068, 591, 1102, 634), 47924, 1 0xBB34 (47924)

```

Figure 3. 3 Core ground truth file example

The first several lines in core ground truth files contain page level information, including the coordinates of the bounding box for the content, page size, resolution, and fonts. After this header, we enumerate the ground truth in a tree structure. Each item of ground truth is listed beginning with its category label, such as zone, line, or char for character item. Following the label is coordinate information of the bounding box in parenthesis, and additional metadata such as a “T” for a text zone, or an “F” for a figure (or non-text zone). All the children items belonging to a parent item follow it in read order. In each word item, we use an integer number, which corresponds to the font (described above), as the property of the word item. For each character item, we provide the character in decimal Unicode, in hex Unicode, and the glyph index as the properties after the coordinate information.

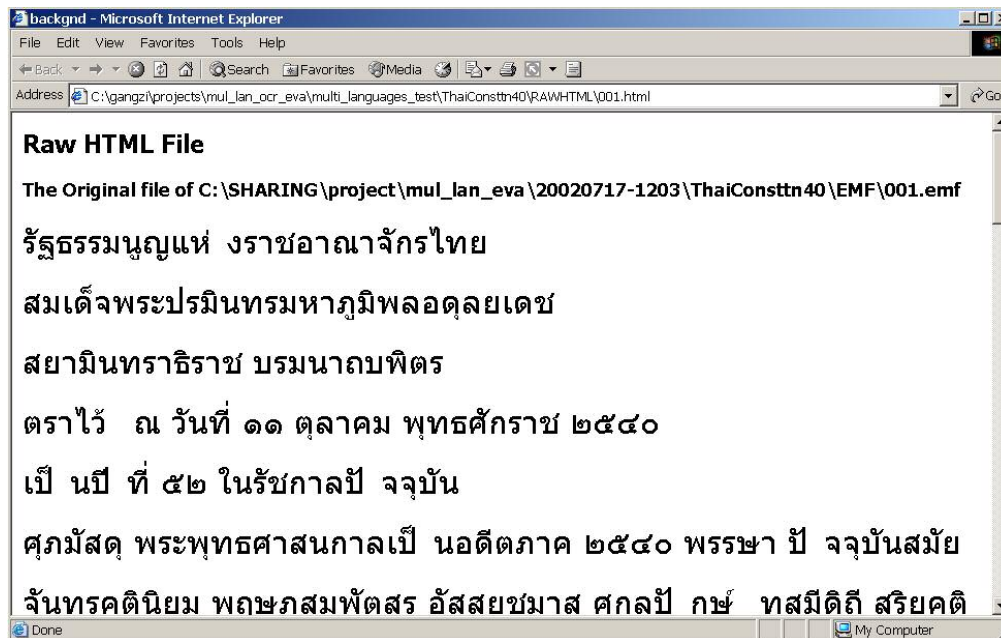


Figure 3. 4 HTML ground truth file example for Thai

The user can check the correctness of obtained ground truth by comparing this HTML file with the original document, assuming the browser correctly renders Unicode.

The synthetic images are noise-free images in different resolutions. Those images can be synthetically degraded by our degradation tool, or physically degraded by printing, coping, faxing, and scanning, as shown in the next chapter. The synthetic images and degraded images can be used to evaluate OCR systems.

### **3.2.1 Obtaining ground truth files from the enhanced meta files**

All the ground truth files are parsed from the Enhanced Meta File (EMF), which consists of a sequence of recorded GDI commands covering all major areas of GDI functions [25]. EMF is used as a generic graphics data exchange format that supports all major elements of graphics, including pixels, lines, curves, texts and bitmaps. Our major goal is to extract all the symbols in Unicode and the position information for each character from the EMF file. The Unicode provides a unique number for every character, independent of the platform, the program, or the language [26]. The ground truth in Unicode can be compared with OCR output, which should be in Unicode also. If the OCR output is in another encoding, say in GB2312 for Chinese, we need to translate the OCR output into Unicode or use the raw files generated from GTG. The position information is the coordinates of the bounding box for each symbol, and can be used to parse the word, line, or zone positions. This higher-level information is critical in evaluating the document segmentation systems.

We use a custom printer driver to get the binary EMF files from structured text documents. Figure 3.5 shows example records in an EMF file.

```
HEADER
    rc1Bounds=(359,281,1311,383)
    rc1Frame=(0,0,21300,27300)
    dSignature=0x464D4520
    nVersion=0x00010000
    nBytes=33860
    nRecords=98
    nHandles=6
    sReserved=0
    offDescription=108
    nPalEntries=0
    sz1Device=(2520,3220)
    sz1Millimeters=(213,273)
    cbPixelFormat=0
    offPixelFormat=0
    bOpenGL=0
EXTCREATEFONTINDIRECTW
    ihFont=1
    elfw.elfCulture=522
    elfw.elfFullName=
    elfw.elfLogFont.lfCharSet=0
    elfw.elfLogFont.lfClipPrecision=64
    elfw.elfLogFont.lfEscapement=0
    elfw.elfLogFont.lfFaceName=Arial
    elfw.elfLogFont.lfHeight=-42
    elfw.elfLogFont.lfItalic=0
    elfw.elfLogFont.lfOrientation=0
    elfw.elfLogFont.lfOutPrecision=4
    elfw.elfLogFont.lfPitchAndFamily=34
    elfw.elfLogFont.lfQuality=0
    elfw.elfLogFont.lfStrikeOut=0
    elfw.elfLogFont.lfUnderline=0
    elfw.elfLogFont.lfWeight=400
    elfw.elfLogFont.lfWidth=0
    elfw.elfMatch=1228892
```

Figure 3.5 EMF file example

A parser written in VC++ is used to extract the information from EMF records. Following are the corresponding records used in our parser:

- **HEADER**

From this record, we can obtain the page size, image resolution, and the content rectangle in mm units.

- **EXTCREATEFONTINDIRECTW**

This record provides the font information and font properties, such as font face name, character set, font height, and whether it is italic or underlined. This record is very important in case of glyph indices used in records of EXTTEXTOUTW instead of Unicode. Once we know the font, we can retrieve the corresponding Unicode using the glyph indices via the mapping file. The character set information helps us to get the original code points other than the Unicode. For example, although most of Chinese documents are coded in Unicode, we may still need GB2312 code points for evaluating OCR software if the OCR only outputs GB2312 code points.

- **EXTTEXTOUTW**

With this record, we can have the coordinate information of each bounding box for the string, the code point of each character, and the offset for characters. By checking the bit of “emrtext.fOptions” value, we can determine whether the following code points are in Unicode or just glyph indices.

If those codes are in Unicode, we are almost done. If they are glyph indices, we need to map them to corresponding Unicode, which will be covered in detail in the next section.

### **3.2.2 Font mapping files and parser tools**

Glyph indices are decoded in the font files, and used to inform the operating system how to draw characters on screen or the printer how to print them. Each font has its own structure, and definition of glyph indices.

Even for the same character in one language, different font files can have different corresponding glyph indices, and different glyph images. Table 1 shows the

different Unicode sequence for the same characters in Urdu language. From this table, we can see that TITUS Cyberbit Basic treated both characters in isolated form, which is not useful for Urdu. Arial Unicode MS treated them partially correct, but does not provide the right ligature. Only Urdu Naskh Asiatype obtains the correct ligature in this case.

Character	Font	Glyph Index	Unicode
ن	Urdu Naskh Asiatype	302	0x06D2 0x0646
ن	Arial Unicode MS	1342 50860	0x06D2 0xFEE7
ن	TITUS Cyberbit Basic	2460 2289	0x06D2 0x0646

Table 1 Example of same character in different fonts

As far as we know, characters and glyphs have three mapping relationships:

1. One to one mapping. One character is represented by a single glyph, and one glyph represents a single character. This is common in languages with large character sets, such as Chinese and Korean. In this case, we can easily retrieve the Unicode from glyph index.
2. One to many mapping. In this case, a character may be represented by a combination of several glyphs, or one character has more than one presentation form. An example for the former case is shown in Figure 3.6, where a character in a Hindi document is composed of glyph 128, and glyph 87. Glyph 87 can be used in other glyph composites as well. For this case, we must retrieve all components of the character, and find all corresponding Unicode code points.



Figure 3. 6 Composition of one character from several glyph indices

The case of multiple forms for one character is common in Arabic documents, where contextual glyph forms are heavily used. There are four forms, initial, middle, final, and isolated, for the same character, depending on the context. For example the character “ha” in Arabic can be represented in four forms, as shown in Figure 3.7.



Figure 3. 7 Arabic character “ha” in isolated, initial, middle, and final form

3. No explicit mapping from glyph index to Unicode. For example, Devanagari, the language used in India, only has 128 code points, from 0x0900 to 0x097F in Unicode table, but has lots of different forms. Using 0x094D, VIRAMA in Hindi language, we can get the half consonants from the full consonant. Using 0x200C and 0x200D, we can get the conjuncts of consonants in different formats. In Hindi fonts, lots of composites are also used. Some of the composites have corresponding Unicode, but not all of them. For those that don’t, we need to provide the Unicode manually.

We use a program “tfdump” to access the internal components of the font file. A typical dumped font file is shown in Figure 3.8

In a font file, “cmap” contains this information. Usually, there is more than one sub-table in “cmap” section. The sub table with “Platform ID 3” and “Specific ID 1” is for Windows OS Unicode. Other sub-tables are used for other operation systems and other coding systems. We used Windows Unicode sub-table in our groundtruth generator system. For detailed information about the font file structure, please refer to [27].

In this sub table, we can find the Unicode character to the corresponding glyph index. For most of the language fonts tested, we can get complete glyph index to Unicode mapping. For other languages, such as Arabic and Hindi documents, we need to get more information from other parts of font file.

```

; TrueType v1.0 Dump Program - v1.63, Apr 11 1996, rrt, dra, gch, ddb, lcp
; Copyright (C) 1991 ZSoft Corporation. All rights reserved.
; Portions Copyright (C) 1991-1995 Microsoft Corporation. All rights reserved.

; Dumping file 'C:\gangzi\project\font\program\font_table_new\font_table_c\test\wingding.ttf'

Offset Table
-----
sfnt version:      1.0
numTables =       18
searchRange =     256
entrySelector =   4
rangeShift =     32

0. 'DSIG' - chksm = 0x4A66FCEE, off = 0x00012858, len = 5136
1. 'LTSH' - chksm = 0x3939391A, off = 0x00001E18, len = 230
2. 'OS/2' - chksm = 0x31C6E48A, off = 0x000001A8, len = 86
3. 'VDMX' - chksm = 0xF374DAB3, off = 0x00001F00, len = 3004
4. 'cmap' - chksm = 0x3BEFC73C, off = 0x00001950, len = 768
5. 'cvt ' - chksm = 0xAE2FA9A9, off = 0x00003270, len = 1338
6. 'fpgm' - chksm = 0xC4F43BB0, off = 0x00002E10, len = 1119
7. 'gasp' - chksm = 0x0823000A, off = 0x00000200, len = 20
8. 'glyf' - chksm = 0xFEFC43883, off = 0x0000509C, len = 52534
9. 'hdmx' - chksm = 0xEE699DA1, off = 0x00003B34, len = 5480
10. 'head' - chksm = 0xC9876654, off = 0x0000012C, len = 54
11. 'hhea' - chksm = 0x12130A8E, off = 0x00000164, len = 36
12. 'hmtx' - chksm = 0x49428A89, off = 0x000037AC, len = 904
13. 'loca' - chksm = 0x25BAEF7C, off = 0x00001C50, len = 454
14. 'maxp' - chksm = 0x0356062A, off = 0x00000188, len = 32
15. 'name' - chksm = 0x81A52B9D, off = 0x00000214, len = 5947
16. 'post' - chksm = 0x596C3A57, off = 0x00011DD4, len = 2692
17. 'prep' - chksm = 0x4FC7275F, off = 0x00002ABC, len = 852

'cmap' Table - Character To Index Map
-----
Size = 768 bytes
'cmap' version: 0
numTables: 2

```

Figure 3. 8 Example of a dumped font file

We have a font parser to automatically generate the font mapping files.

Following is the pseudo code we used in font parser program:

```

While ( fontfile is not end)
{
    switch ( glyph_index_type )
    {
        case one_to_one:
            add_oneNode ( glyphIndex, Unicode);
            break;
        case composite:

```

```

        Unicode = find_composite(glyphIndex);
        If (Unicode == NULL)
            Record_error(glyphIndex);
            Draw_glyph(glyphIndex);
        else
            Add_oneNode( glyphIndex, Unicode);
    }
}

```

Using our font parser tool, two output files and one directory are obtained for each font file: the font mapping file, the font verification file and the glyph images directory. The font-mapping file is used by the ground truth generator to retrieve the Unicode from the glyph index if necessary. The font verification file is written in the HTML file, and is used to check the correctness of the font-mapping file. Because the font for each cell in the HTML file can be specified individually, we can compare the glyph image, which is the image extracted from font file directly, with the image generated from the Unicode under that font file. Figure 3.9 is an example of a font verification file for Devanagari language.

The first column is the glyph indices ranked in ascending order; while the second column is the Unicode candidate in Hex format if available. If we could not find the Unicode candidate for this character in the font file, a “NULL” label is put there to remind us to map this index to Unicode manually later. The real glyph image for that index is put in the third column. The forth column is the image generated by the Unicode candidate under the specific font, say Mangal in this example, which is a Unicode font for Devanagari language.

Once all the “NULL” indices have been mapped manually, this font verification file can be generated again to check the correctness of manual patches.



Figure 3. 9 Example of font verification file for Mangal font

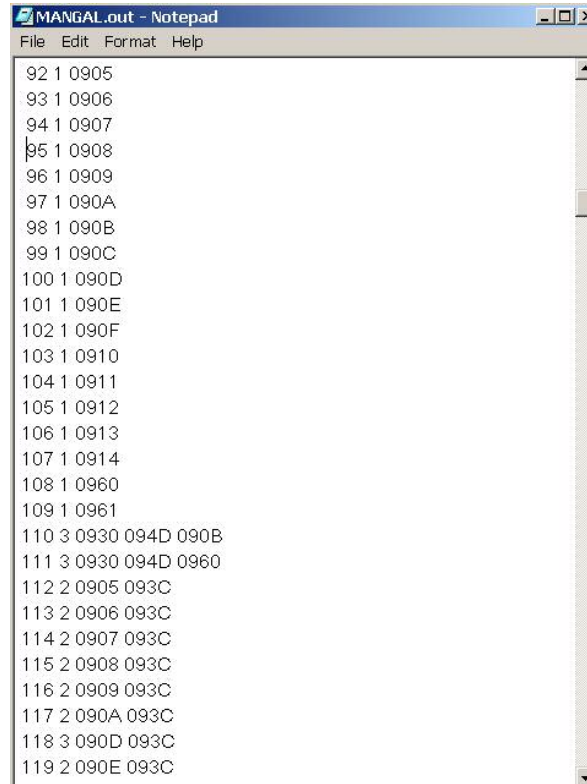


Figure 3. 10 Example of font mapping file for Mangal font

Figure 3.10 shows an example of a finished font-mapping file, from which we can see that the glyph index 110 has been decoded.

Once we decoded all the font information, and have the glyph indices from EMF file, we can obtain the ground truth file in Unicode and in original coding page by mapping the glyph index to Unicode.

### 3.3 Evaluation tools

The algorithm in [28] is employed to evaluate the performance of underlying OCR systems. Three kinds of error are defined according to three types of edit operations on the string: deletion, insertion, and substitution errors. For example:

```
Ground truth:      comparison
OCR output:       c mtarisonkj
Operations:       -I-S-----DD
* Where I: Insertion S: Substitution D: Deletion -Correct Recognition
  The accuracy in this example is 80%
```

We have ported the code from UNIX [29], and integrated it into our evaluation system. Character level and word level accuracy reports are calculated page by page. A summary is reported for the whole document and a collection; while accuracy confidence intervals are computed from the accuracy rates.

For visualization, we have used a scatter plot to compare between two OCR runs. A diagram of sorted accuracy reports for different OCR runs is used first time in our evaluation to show the recognition pattern of systems. Knowing which patterns are the most vulnerable in recognition will help improve the classifier.

Figure 3.11 is the screen shot of our evaluation tool interface. The user can choose the underlying OCR output files and the ground truth files from this interface. Depending on the amount of OCR'd data, our system can generate OCR profiles

from: structured folders, two directories, or two pages. Using a structure folder, we can process thousands of OCRed pages. Using two directories, we process the OCRed files and the ground truth files in two separated directories.

For the user's convenience, the OCRed file name need not be the same as the ground truth file. Thus a different prefix or suffix can be used to distinguish different OCR software or different degradation levels, methods etc. To align the OCRed file with corresponding ground truth files, users can specify the alignment file, use the file name, or even let them be processed alphabetically.

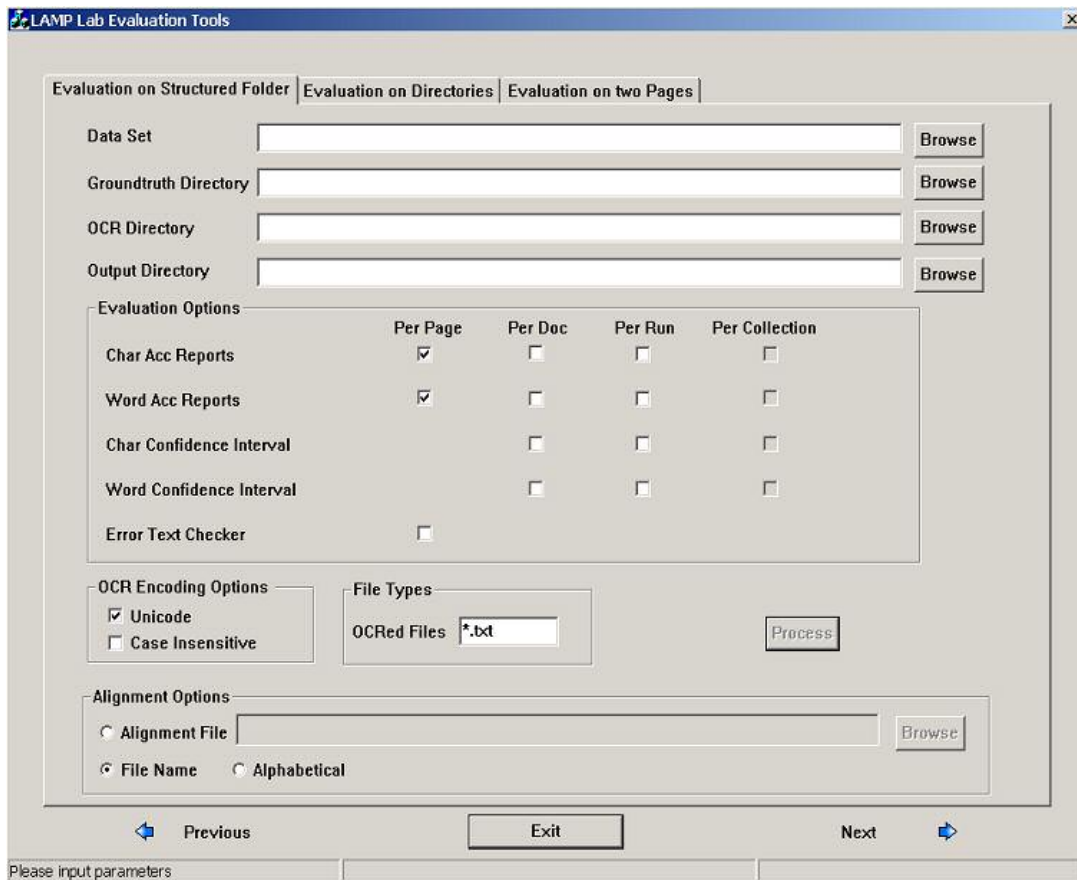


Figure 3. 11 Screen shot of evaluation system interface

### 3.4 Evaluation examples

Two primary Chinese OCR systems, OCR1 and OCR2, are tested in our evaluation experiments. We adopt the black box method here.

We used the available United Nations' Anti-Chemical Weapon Treaty, and other documents in our evaluation. This treaty is in six different languages: Arabic, Chinese, English, French, Russian, and Spanish.

The performances of the OCR systems are evaluated as follows. First the ideal images and ground truth files are generated by GTG from electronic text. Second, the noise-free images and degraded images, including the physically scanned images and synthetically degraded images, are input to the OCR systems. To get the scanned images, we printed out the document, and scanned it back in 200dpi, 300dpi, and 400dpi.

Then the OCR results from noise-free images and scanned images are compared with the ground truth files. Since the output of both systems is in GB2312, the raw files in original encoding are used. Finally, the accuracy rate is calculated page by page, and the overall evaluation results are obtained from those rates.

Figure 3.12 shows the accuracy scatter diagram of the two OCR systems using the 100 dpi and 300 dpi noise-free images. The horizontal axis represents accuracy rate from one of the OCR runs, while the vertical axis represents accuracy rate from the other OCR run. The coordinate of each circle in this diagram represents the accuracy rate pair of the two OCR runs for each page in the data set. The x-coordinate corresponds to the OCR2 accuracy for that image and the y-coordinate corresponds to the OCR1 accuracy. For example, if OCR2 obtained 49.46% accuracy rate, while OCR1 obtained 92.43% for one page, then the coordinates of circle should

be (49.46, 92.43) in diagram. From this example, we can see that OCR1 outperforms OCR2 on almost all pages.

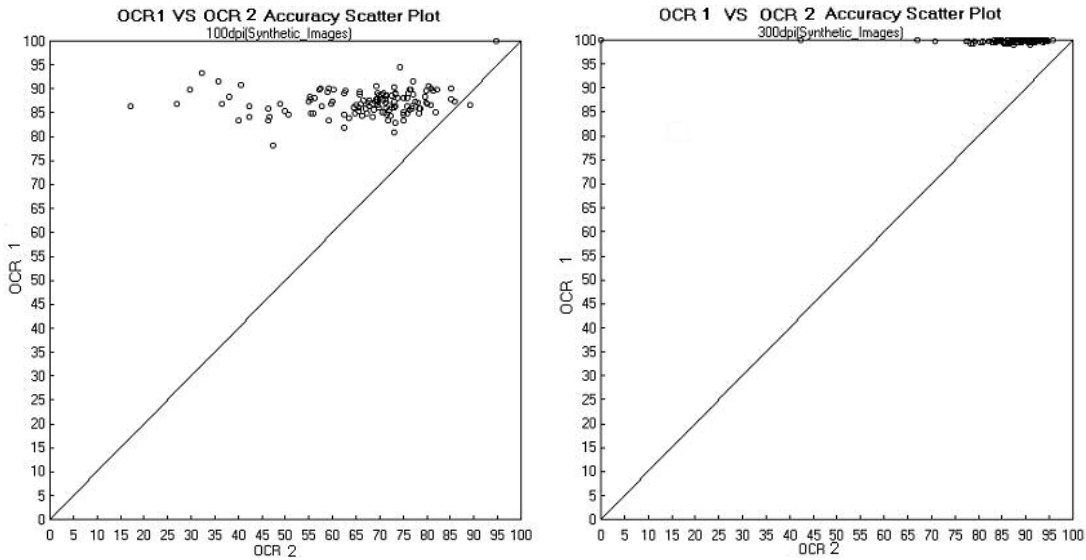


Figure 3. 12 Accuracy scatter plot for two OCR with synthetic images

Figure 3.13 shows the overall performance for physically scanned images at different resolutions. Calculating the accuracy rate over all pages will give us more accurate and more comprehensive analysis for the OCR software.

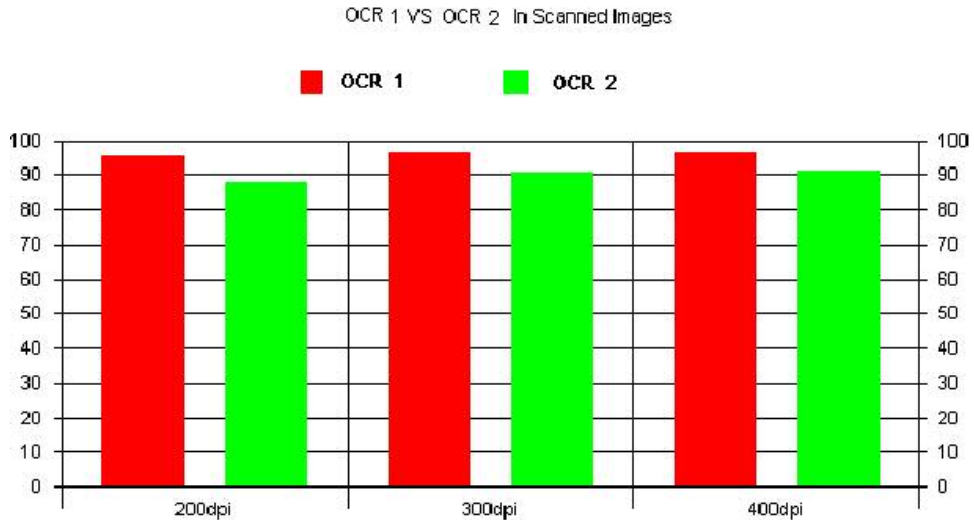


Figure 3. 13 Overall performances diagram for two OCR with scanned images

Figure 3.14 shows sorted OCR accuracies. We sorted the accuracy rates for each OCR run, and displayed them in this graph. From this Figure, we can easily see the highest accuracy rate, lowest accuracy rate, and performance pattern for each run.

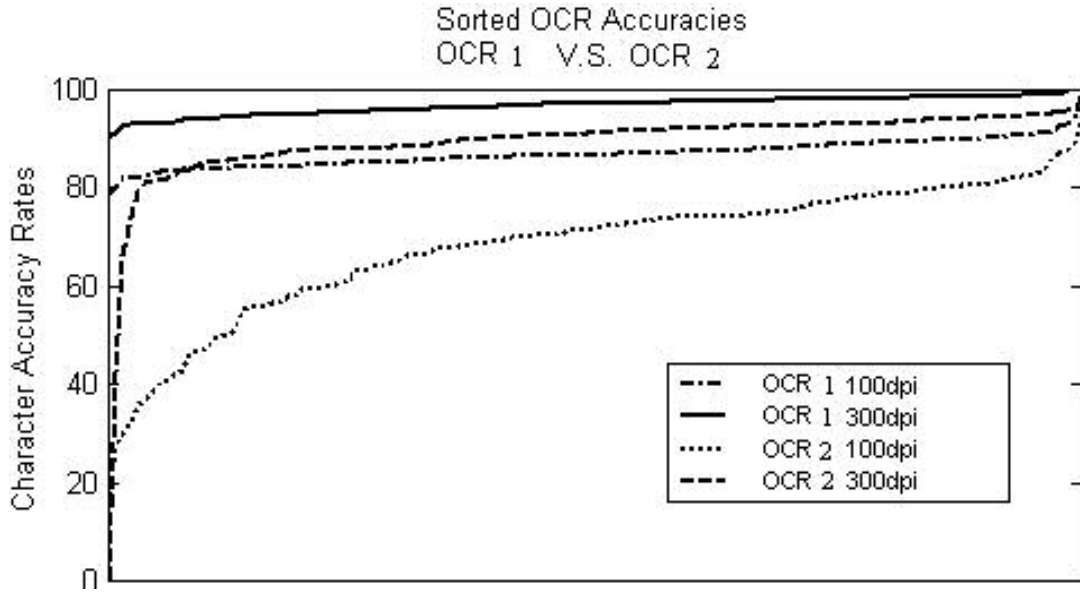


Figure 3. 14 Sorted accuracy rate in different runs

Figure 3.15 is the accuracy scatter plot for the synthetically degraded images at different noise levels. Two levels of DDM [6] degraded images were used here to test our OCR systems. The high noise level images are generated by using the parameters ( $C_0=0, \alpha_0 =1.0, \alpha= 0.5, \beta_0 =1.0, \beta = 2.5, \gamma=3$ ), and the lower noise level images are generated by using ( $C_0=0, \alpha_0 =1.0, \alpha= 0.5, \beta_0 =1.0, \beta = 2.5, \gamma=2.0$ ). From this diagram, we can see that the performance drops as the noise level increases.

Tables 2 and 3 are the percentage accuracy summaries (accuracy and confidence intervals) for ideal, physically scanned images.

	OCR1		OCR2	
	100dpi	300dpi	100dpi	300dpi
ACC Rate	86.89%	99.82%	65.54%	88.95%
ACC Stat	86.52~87.27	99.78~99.85	63.09~67.97	88.23~89.68

Table 2 OCR Performance for synthetic images

	OCR1			OCR2		
	200dpi	300dpi	400dpi	200dpi	300dpi	400dpi
ACC Rate	95.64%	96.25%	96.43%	87.89%	90.55%	91.05%
ACC Stat	94.65~96.67	95.46~97.07	95.64~97.26	86.23~89.58	88.83~92.33	89.30~92.85

Table 3 OCR Performance for scanned images with different resolutions

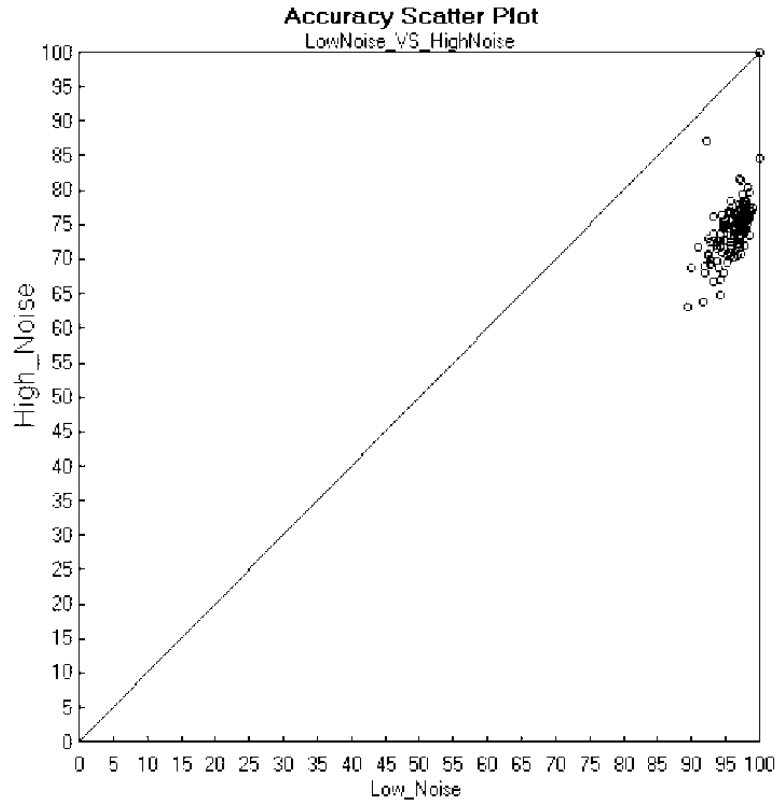


Figure 3. 15 Accuracy scatter plot for one OCR with two noise level images

## Chapter 4 Ground truth alignment

Degraded images with its original electronic text content are often a suitable test bed for OCR since many evaluation methodologies work by aligning entire passages of text. In some cases, however, character, word and line locations are still necessary. The coordinate information is helpful in evaluating the segmentation and layout analysis capability of OCR system for example, while the fonts, and character size information maybe useful in training OCR classifier. Unfortunately, after the documents are printed, copied, and faxed or rescanned, the original ground truth location is typically no longer aligned with the degraded images. In this chapter, we will discuss a methodology to align noise free images to the degraded images in order to obtain the ground truth files for those degraded images.

In [5], the author modeled the geometric transformation of the scanned images via a linear transformation matrix. This linear transformation assumption includes rotating, scaling, shearing, and translating. Using this model, we have obtained reasonable results in aligning images taken from a digital camera, or from a print-fax-scan procedure. If there is a nonlinear factor in the degradation procedure, our system can still provide a coarse bounding box for further local adjustment.

### 4.1 Alignment overview

Figure 4.1 shows the alignment procedure.

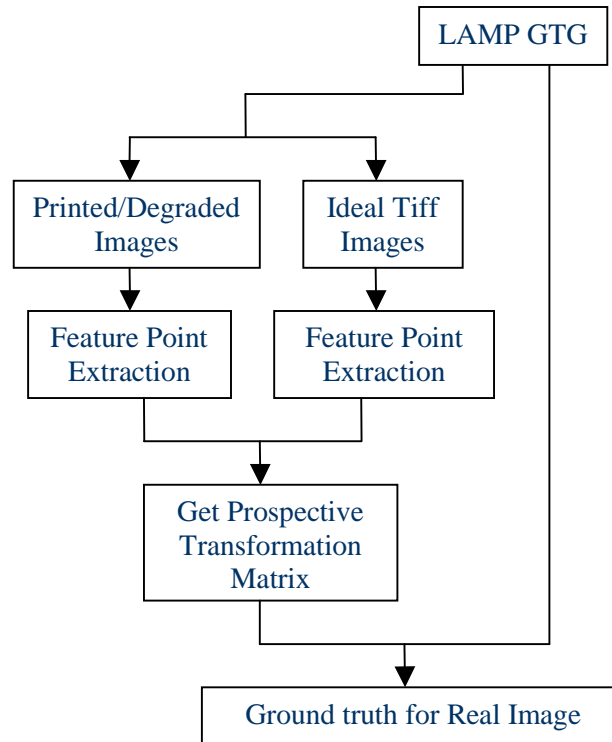


Figure 4. 1 Noise free image and degraded image alignment procedure

The following is the detailed procedure to get the linear transformation matrix.

1. Obtain ideal images with ground truth from our GTG. Unlike the use of the four outermost points of all the bounding boxes of connected components on the images in [5], we put four disks in 14 points at the “Header and Footer” position of each page. Disks are used in our experiment for two reasons. The first is that with dots we can easily find the geometric center from the coordinate of bounding box even if it degraded to an ellipse. The second is that we can detect an ellipse much easier than detecting a cross using connected component methods.
2. Obtain the degraded images by printing the ideal images, copying them, and faxing them, for example. Figure 4.2 shows the example of a noise free image and the corresponding faxed image.

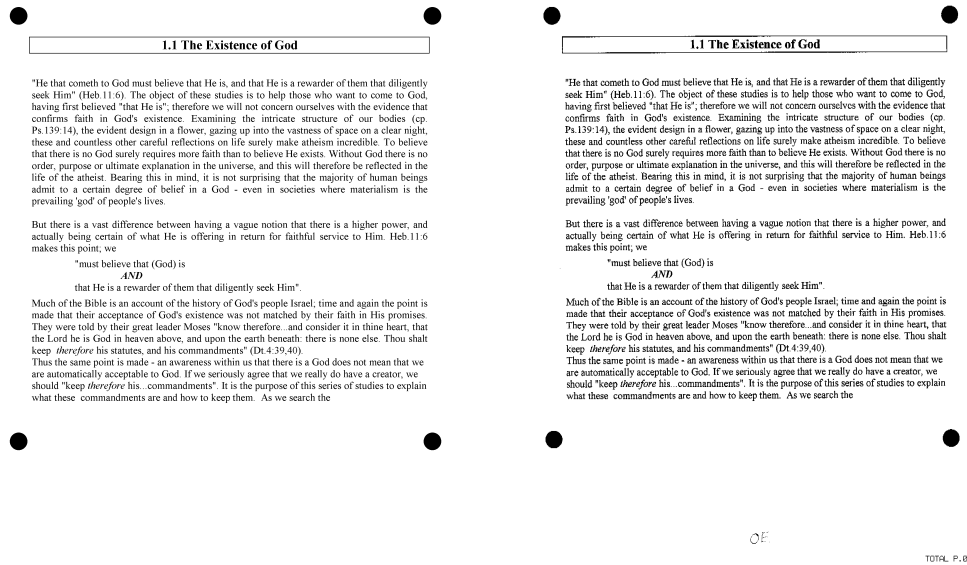


Figure 4. 2 Noise free image and faxed image example

3. Locate feature points in the ideal images and the corresponding degraded images. The position of each feature point on the noise free images and degraded images are detected by the pattern of disks. Following is the program used to locate those feature points.
  - Connected components are calculated on the image. Those with too small or with large ratio of length to width are discarded as noise.
  - All components are checked to find feature points. Here we used the fact that the ratio of area over the multiplication of length and width of an ellipse should be a constant  $\pi$ . If the ratio is close to  $\pi$ , we can label the connected component as the feature points.
  - The position of each feature point is determined by simply computing the geometric center of the bounding box of detected disk or ellipse.
4. Compute the mapping matrix by the feature point pairs. The projective transformation matrix is calculated by:

$$\begin{pmatrix} x \\ y \end{pmatrix} = \frac{1}{w} \begin{pmatrix} p_1u + p_2v + p_3 \\ p_4u + p_5v + p_6 \end{pmatrix}$$

$$w = \frac{1}{p_7u + p_8v + 1}$$

Where (x, y) is the coordinates of the feature point on the ideal image, (u, v) is the coordinates of the feature point on the degraded image.  $P_i$ s are the coefficients of the transformation matrix.

5. We can align the ground truth for noise-free image to degraded images by the calculated transformation matrix.

## 4.2 Alignment experiments

To test our alignment methodology, we printed those ideal images and scanned them in four combinations non-skew/skewed and shrink/enlarge. Figure 4.3 shows an example of a skewed and shrunk English document, and a skewed and enlarged Chinese document.

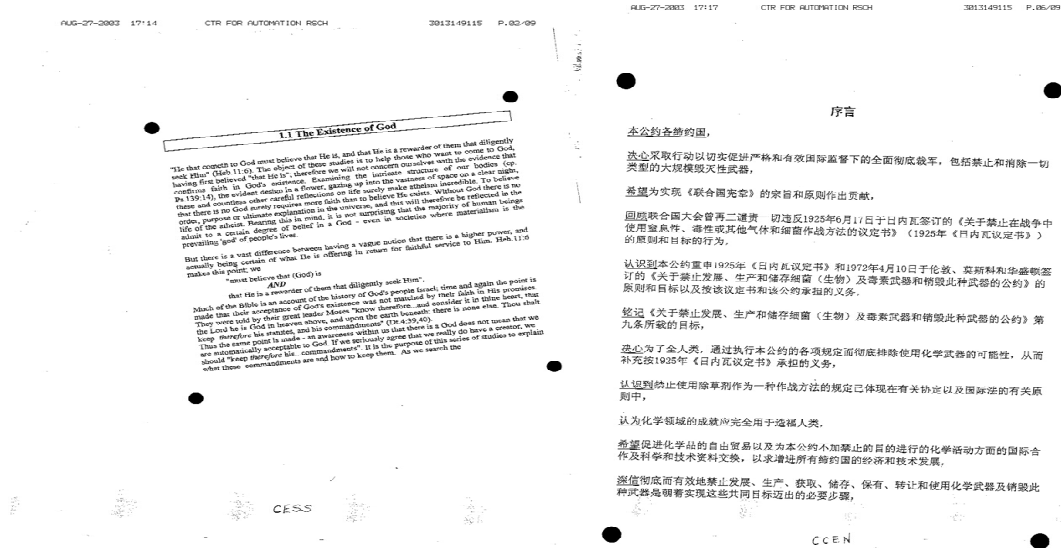


Figure 4.3 Example of skew and shrink/enlarge document example

Figure 4.4 shows an example of a faxed English document with the computed bounding boxes displayed on it.

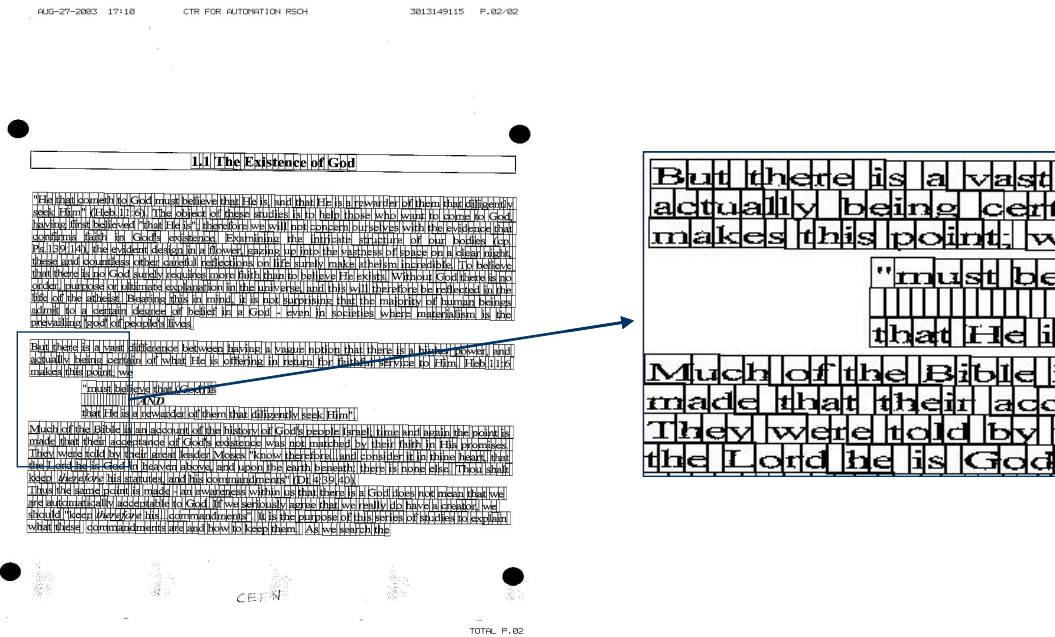


Figure 4. 4 Example of aligned English document

Figure 4.5 shows an example of a faxed Chinese document with the computed bounding boxes displayed on it.

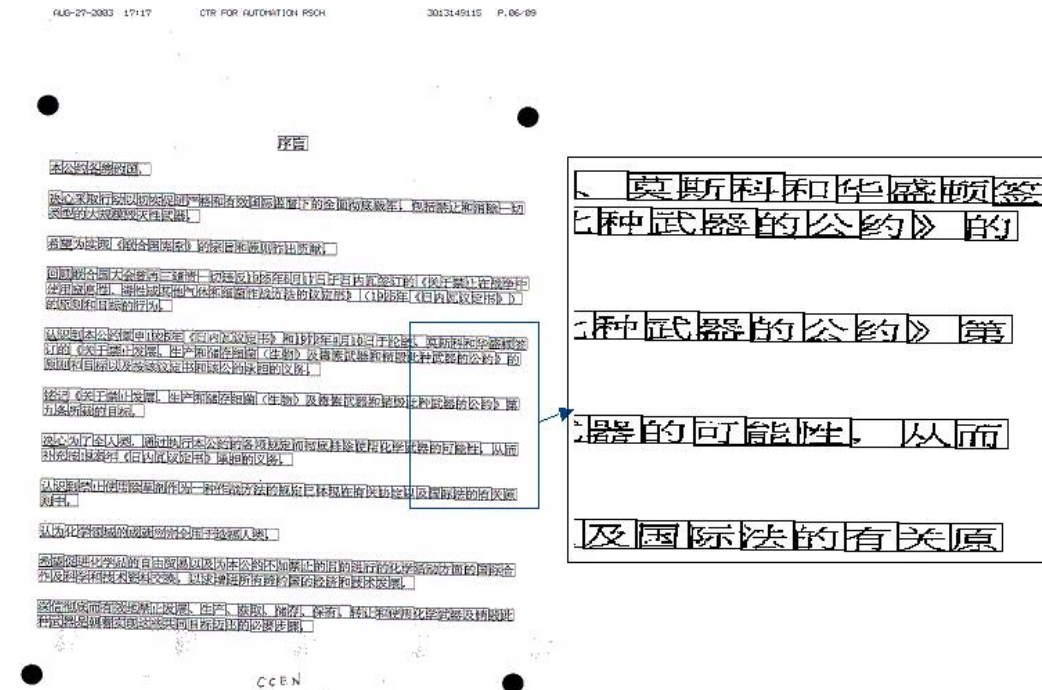


Figure 4. 5 Example of aligned Chinese document

We also tested our alignment system with document images obtained from a digital camera with perspective distortion. Figure 4.6 and 4.7 are document image from camera and the computed bounding boxes respectively.

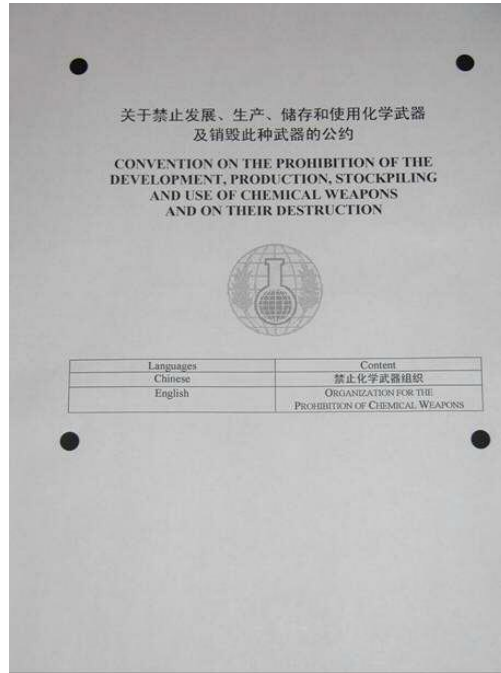


Figure 4. 6 Document image with complex content from camera

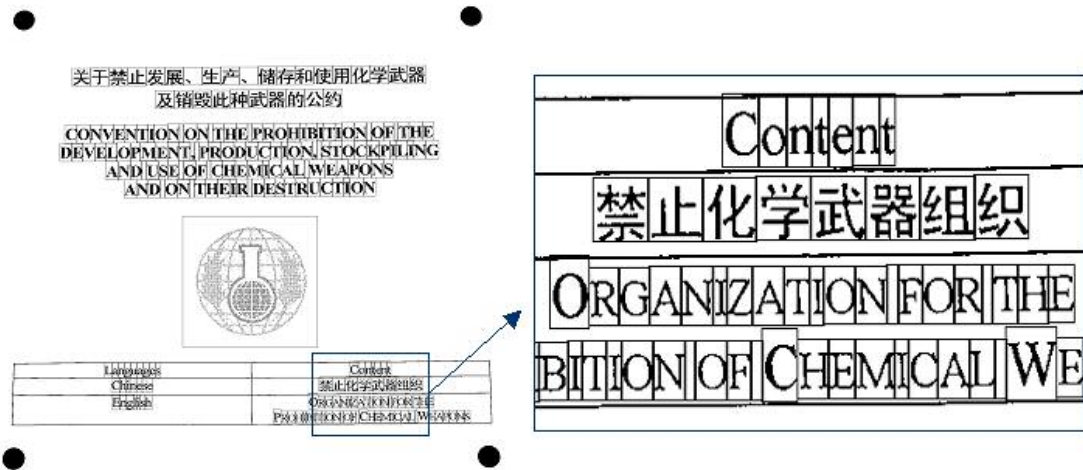


Figure 4. 7 Example of aligned camera image

## Chapter 5 Document image degradation

In this chapter, we present a method to generate synthetic noisy images at both page and pixel levels. The main components of our system and the types of noise are explained in detail in following sections.

### 5.1 Image degradation architecture:

The architecture of our system is shown in Figure 5.1.

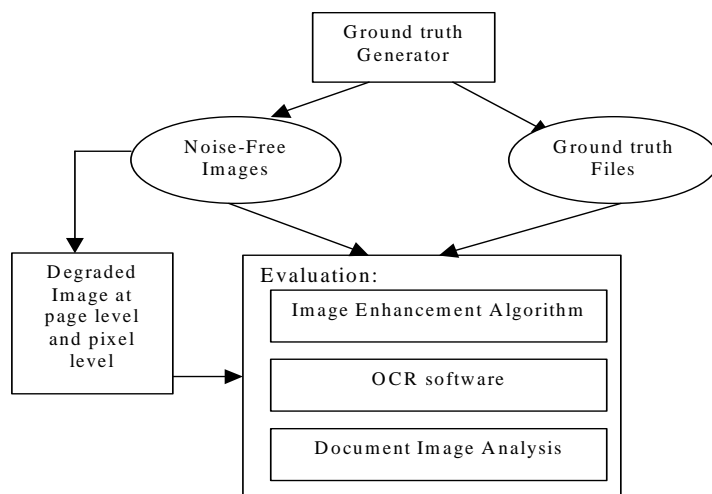


Figure 5. 1 Image Degradation and Application Architecture

Beginning with electronic text, the ground truth generator can produce noise-free images and corresponding ground truth files by using custom printer driver and metafile information. Degraded images can then be obtained physically by printing, copying, faxing, and scanning, or synthetically by using degradation methods.

To make our degradation method effective, while as simple as possible, we choose several types of noise of greatest interests. Some of them have been presented in [17]. For page level noise, we have rotation, blur, lines, resolutions change, and additive noise templates. For pixel level degradation, we add speckles, jitter, and

pixel drift to the document. We have also studied the show-through and bleed-through in this chapter.

## 5.2 Page level noise

Skew, or rotation, is common in scanned or faxed documents. We have implemented two methods for skew. The first one takes the rotation angle as the input, rotates the given image at the center of the image, and resizes the image if necessary. Alternatively, the user can choose the pivot and rotation angle.

In general, we can express the spatial transformation, including rotation and skew, using a polynomial function:

$$x = \sum_{i=0}^N \sum_{j=0}^N m_{ij} u^i v^j$$

$$y = \sum_{i=0}^N \sum_{j=0}^N n_{ij} u^i v^j$$

where  $x$ ,  $y$  and  $u$ ,  $v$  are coordinates in the input and output images, respectively;  $N$  is the polynomial order, and  $m$ ,  $n$  are coefficients, which can be computed from the registered point pairs of input and output images. When  $N=1$ , it is bilinear interpolation:

$$x = m_{00} + m_{01}v + m_{10}u + m_{11}uv$$

$$y = n_{00} + n_{01}v + n_{10}u + n_{11}uv$$

In our method, we use the nearest-neighbor interpolation because it is faster and accurate enough for binary document images.

Figure 5.2 shows the effect of two kinds of rotation. The left one has been rotated  $45^\circ$  at the center of image, and has been resized to adapt the change. The right image has been rotated  $10^\circ$  without changing the size.

Chief Executive to renew ties with our trading partners  
 The Chief Executive, Mr Tung Chee Hwa, will visit Malaysia, Singapore, the United States, Japan, Belgium and the UK in the next two months to renew ties with our trading partners and update them on developments in Hong Kong after the handover. During these visits, Mr Tung will call on political and business leaders, and brief them on the smooth transition in Hong Kong to demonstrate our pride to return to China and our confidence in "Hong Kong people ruling Hong Kong" under the "one country, two systems" concept.  
 Mr Tung will be in Kuala Lumpur on September 3 and call on Prime Minister Dr Mahathir Mohamad.  
 He will be in Singapore on September 4 and 5 and call on Prime Minister Goh Chok Tong.  
 Mr Tung will be in the United States from September 9 to 11. He will visit Washington and New York.  
 In Washington, Mr Tung looks forward to meeting with President Clinton.  
 Mr Tung will also officiate at the opening ceremony of the new office premises of the Hong Kong Economic and Trade Office in Washington.  
 Mr Tung will be in Tokyo from October 15 to 17. He will call on ministers, parliamentarians and senior officials of the Japanese Government.  
 He will then leave for Europe on October 19 and visit Brussels and London before returning to Hong Kong on October 23.

Chief Executive to renew ties with our trading partners  
 The Chief Executive, Mr Tung Chee Hwa, will visit Malaysia, Singapore, the United States, Japan, Belgium and the UK in the next two months to renew ties with our trading partners and update them on developments in Hong Kong after the handover. During these visits, Mr Tung will call on political and business leaders, and brief them on the smooth transition in Hong Kong to demonstrate our pride to return to China and our confidence in "Hong Kong people ruling Hong Kong" under the "one country, two systems" concept.  
 Mr Tung will be in Kuala Lumpur on September 3 and call on Prime Minister Dr Mahathir Mohamad.  
 He will be in Singapore on September 4 and 5 and call on Prime Minister Goh Chok Tong.  
 Mr Tung will be in the United States from September 9 to 11. He will visit Washington and New York.  
 In Washington, Mr Tung looks forward to meeting with President Clinton.  
 Mr Tung will also officiate at the opening ceremony of the new office premises of the Hong Kong Economic and Trade Office in Washington.  
 Mr Tung will be in Tokyo from October 15 to 17. He will call on ministers, parliamentarians and senior officials of the Japanese Government.  
 He will then leave for Europe on October 19 and visit Brussels and London before returning to Hong Kong on October 23.

Figure 5. 2 Example of rotation of 45° and rotation of 10°

Blur is another typical artifact found in degraded images, and is often caused by a point spread effect in printing and/or scanning. This type of noise, along with threshold, significantly affects recognition accuracy of almost any classifier [17]. We can model blur noise by convoluting the image with a Gaussian low pass filter. With our degradation method, the user can specify the Gaussian function's standard deviation  $\sigma$  (in unit of pixels), the size of the spatial smoothing mask, the convolution probability for each pixel, and the threshold value. As shown in Figure 5.3, the 2D Gaussian function has been sampled at equal intervals, and has been normalized to obtain the filter. Because the Gaussian distribution is non-zero everywhere, we truncate the kernel at the point of three standard deviations from the mean. For example, if  $\sigma = 1.0$ , size of mask is 7, a 7x7 matrix will be generated. The element,  $M(u, v)$ , of this mask before normalization can be calculated by:

$$M(u, v) = \frac{1}{2\pi\sigma^2} e^{-\frac{u^2+v^2}{2\sigma^2}}$$

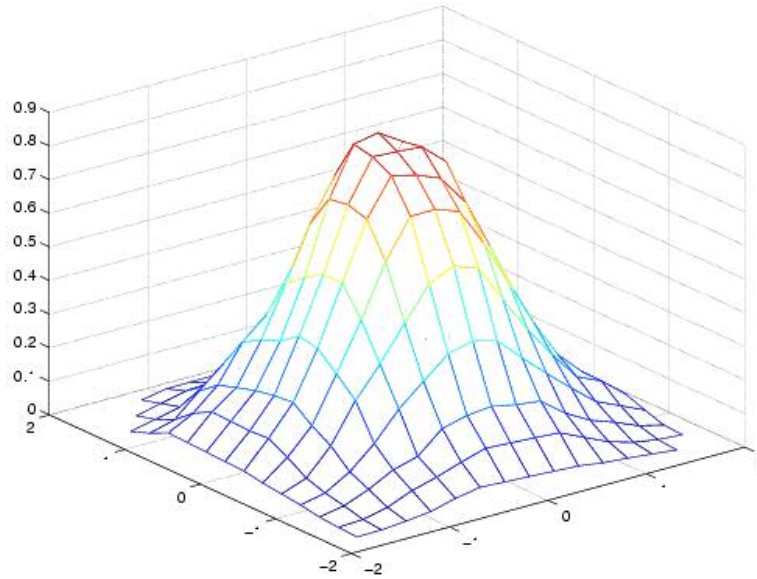


Figure 5. 3 2D Gaussian Function and sampling grid

This 2D convolution is quite slow in processing large images with large masks. However, the speed can be increased by convolving the image with two 1D Gaussian filter on X and Y direction separately because of the separability of Gaussian filter.

For each foreground pixel, the convolution probability will be compared with a uniformly generated random number to determine if the convolution mask should be applied on this pixel. If it should, after the convolution, the threshold will be used to decide if the underlying pixel will be set as foreground or as background. One example of an image before and after blurring is shown in Figure 5.4.

Another important page level noise is the random lines scattered horizontally or vertically on the document image. This happens frequently in the faxed or copied

documents when individual sensors are bad. The parameters of this kind of noise in our model include: the number of lines, the minimum, and maximum of the length, width and density for the lines. Each of the line's length and width will be chosen randomly in the given range, and will be overlaid on the image. The density parameter controls the percentage of black pixels in one line. Not only adding lines to the image, the user can also randomly remove lines from the image. The effect of adding a horizontal line and removing vertical line can be seen in Figure 5.5b and 5.5c respectively.



Figure 5. 4 Example of a document before and after blurring

Merge is used to combine the noise free image with noise templates, which are obtained from the background of physically scanned images or copied images. Using this method, we can create thousands of "scanned" or "copied" test images at minimum cost. Figure 5.6 shows the effect of "additive" merge. Although this method may not be ideal for OCR training and testing, it works well for document image segmentation and analysis evaluation, such as hand written or logo detection

algorithms. Figure 5.6 shows the original image, noise template, and effect of combination of noise template with given image.

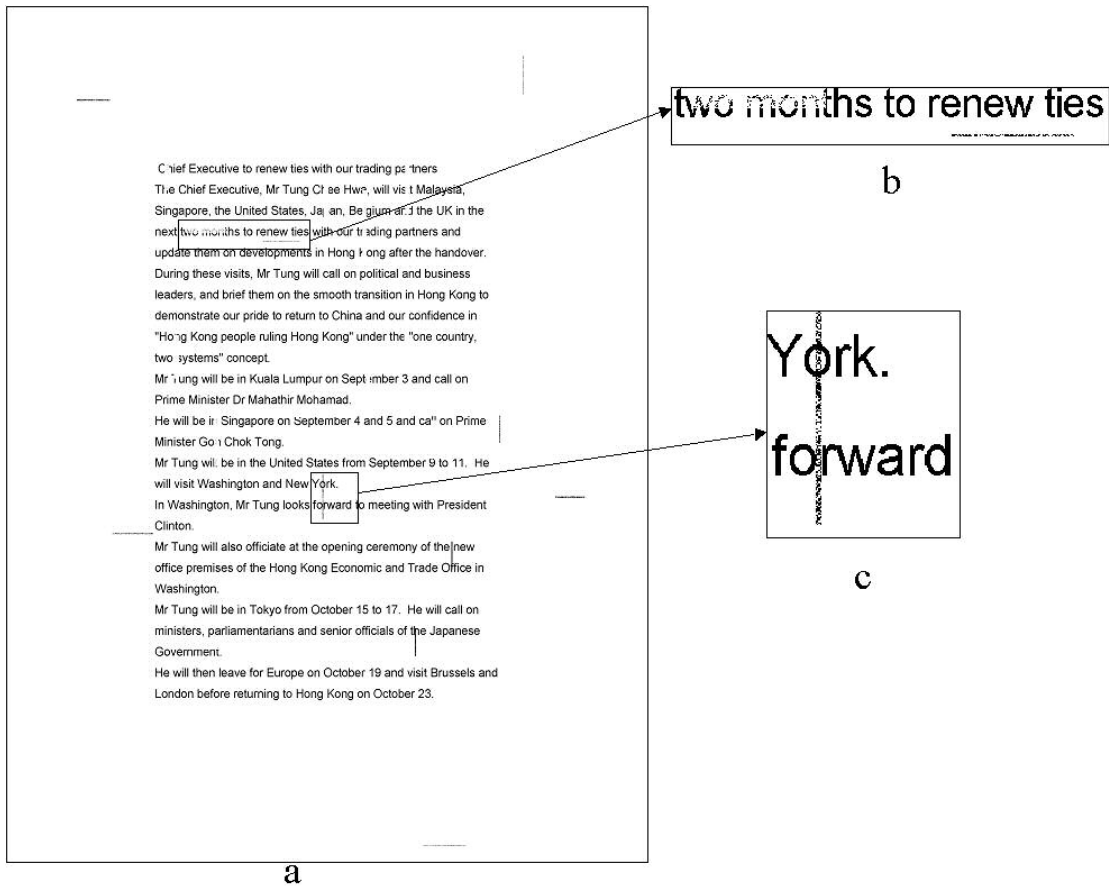


Figure 5. 5 Example of scattering lines on document image

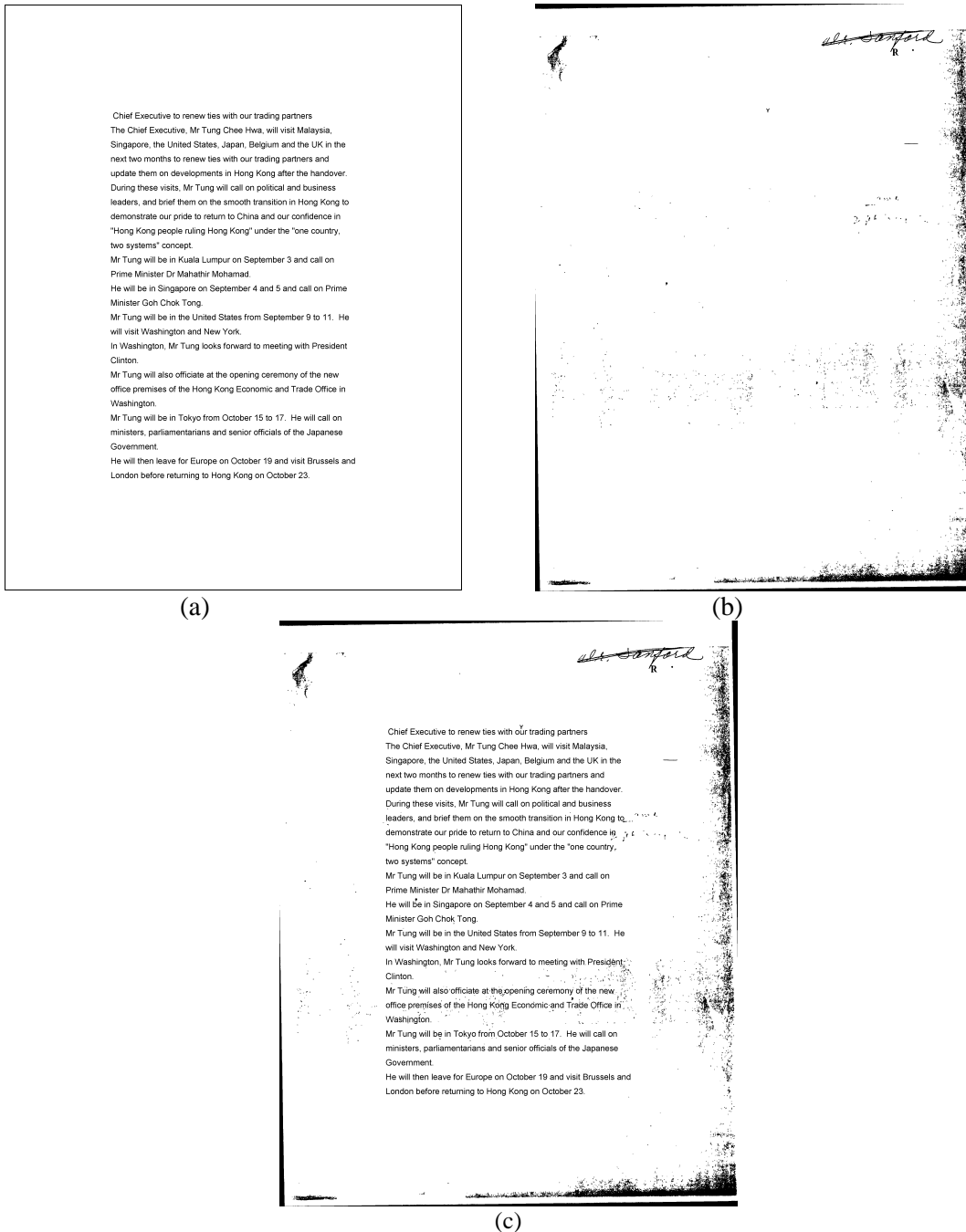


Figure 5. 6 Example of merge (a) noise free image (b) noise template (c) degraded image

### 5.3 Pixel level noise

In addition to the page level noise discussed in last section, several pixel level noise models are presented in this section.

Speckles are multiplicative noise, and can be expressed as:

$$Y(u, v) = X(u, v)(1 + n)$$

where  $X(u,v)$  is the original pixel intensity,  $Y(u,v)$  is the degraded value, and  $n$  is a random number. In our model, we define speckles as the randomly generated patterns with different pixels according to the specific distributions. The effective sizes of patterns can be chosen by the user, and usually defined from 1 to 10. The parameters of this method include the frequencies of each speckle pattern, and the probability of speckle generation, which can control the number of speckles on the image. The frequencies of each speckle size will be used to obtain the distribution of speckles. We use Cumulative Distribution Function (CDF) of the distribution and the uniformly generated random number to generate the speckles distributed according to the given profile.

For example, if the given distribution for speckle with size 1 to 5 is:

Size	1	2	3	4	5
Probability	0.33	0.33	0.16	0.1	0.08

The corresponding CDF is:

Size	1	2	3	4	5
CDF	0.33	0.66	0.82	0.92	1.0

Every time we need to generate a speckle, we choose the “ceil” size number where a random number falls into. For example, if the random number falls between 0.82~0.92, size 4 will be chosen. Because the random number is distributed uniformly, the probability of choosing corresponding speckle size is determined only by the interval of the CDF. Thus the probability of “showing” speckles with size 4 is 0.1 in this example. An example of speckles in different patterns is shown in Figure 5.7c.

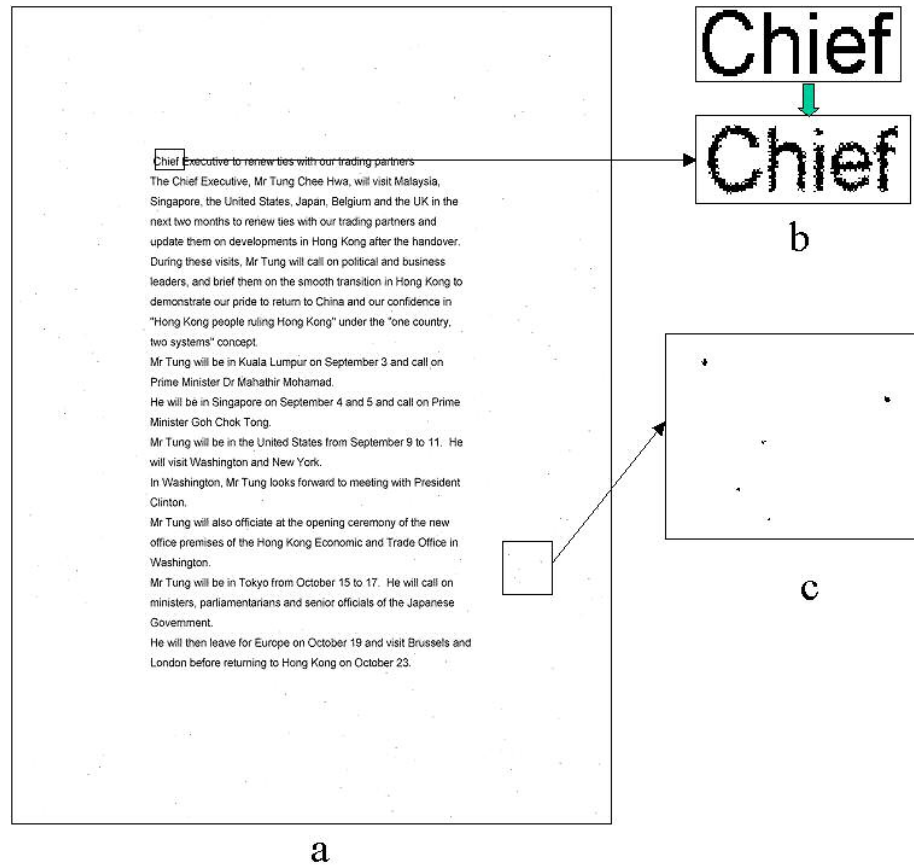


Figure 5. 7 Example of speckles and jitter (a) degraded image (b) jitter effect (c) speckles

Jitter is one of the local noises introduced in our method to mimic the effect of disturbance of sampling grids during copying and scanning. This white noise jitter samples uniformly in the 2D windows with size  $r$  centered at the given pixel, as given by the following function:

$$Y(u, v) = X(u + r_1, v + r_2)$$

where,  $Y(u, v)$  is the new intensity value for pixel at  $(u, v)$ ,  $X(u + r_1, v + r_2)$  is the intensity at  $(u + r_1, v + r_2)$ ,  $r_1$  and  $r_2$  are independent random variables uniformly distributed inside the widow with size of  $r$ .

Jitter will invert the pixels along the edge with higher probability than those in homogeneous regions. Figure 5.7b shows the effect of jitter with  $r = 2$ . This effect is similar, but not the same, to following degradation method, pixel flipping.

Based on the DDM proposed in [5], pixel flipping can invert a given pixel from black to white or vice versa. This method has seven parameters; the first one is the seed used for the random number generator. The following 5 parameters are used in the following function:

$$P(x=1 | x=0, d_1) = P_0 + A_0 \exp(-B_0 d_1^2);$$

$$P(x=0 | x=1, d_2) = P_0 + A_1 \exp(-B_1 d_2^2);$$

where  $P(x=1 | x=0, d_1)$  is the probability of a given background pixel inverted to foreground,  $d_1$  is the distance from background to foreground; while  $P(x=0|x=1, d_2)$  is the probability of a given foreground pixel inverted to background,  $d_2$  is the distance from foreground to background. The effect of pixel drift can be seen in Figure 5.8.

本公约各缔约国，

(a)

本公约各缔约国，

(b)

本公约各缔约国，

(c)

Figure 5. 8 The effect of pixel level degradation. (a) Original image; (b) Degraded in low noise level; (c) Degraded in high noise level.

## 5.4 Bleed-through and show-through noise

### 5.4.1 Background

Bleed-through is often found in many ancient manuscripts and is caused in part by ink seeping from the reverse side of the manuscript. Show-through appears in scanned double-sided printed document images when the paper is not completely opaque, and the light in the scanner is allowed to reflect back through the document.

Figure 5.9 is an example of scanned newspaper.



Figure 5.9 The show-through effect of a scanned newspaper

Although this type of artifact is often encountered in document imaging, existing degradation such as [15] [18], have not explicitly investigated this type of noise. In [31], several synthetic show-through or bleed-through images were generated to test noise cancellation and recovery algorithms. However, to make the data model a noiseless mixture for applying Independent Component Analysis (ICA) methods, the authors assumed no noise or blur, which made the generated images unrealistic. In [32], the author analyzes the show-through phenomenon using first physical principles, and models it with a linear function of reflectance and transmittance. Because his focus was on removing the show-through noise, the author in [32] uses this model to design a linear filtering scheme instead of generating synthetic images.

The necessity and the work aforementioned above have inspired us to incorporate show-through effect into our degradation model, which is described in detail in following section.

#### **5.4.2. Approach**

To obtain an image with show-through effect from a given front side image and a back side image, we reverse the back side image left-to-right, and then blur it with a Gaussian low pass filter. We combine the preprocessed back side image with the front side image to generate the synthetic one.

It is relatively easy when either the front side or the back side image is binary. We threshold the other image into binary if it is grayscale, and apply logical “OR” operator to both binary images. An example of combining a grayscale back side image with a binary front side image is shown in Figure 5.10.

Chief Executive to renew ties with our trading partners  
 The Chief Executive, Mr Tung Chee Hwa, will visit Malaysia, Singapore, the United States, Japan, Belgium and the UK in the next two months to renew ties with our trading partners and update them on developments in Hong Kong after the handover. During these visits, Mr Tung will call on political and business leaders, and brief them on the smooth transition in Hong Kong to demonstrate our pride to return to China and our confidence in "Hong Kong people ruling Hong Kong" under the "one country, two systems" concept.

Mr Tung will be in Kuala Lumpur on September 3 and call on Prime Minister Dr Mahathir Mohamad.

He will be in Singapore on September 4 and 5 and call on Prime Minister Goh Chok Tong.

Mr Tung will be in the United States from September 9 to 11. He will visit Washington and New York.

In Washington, Mr Tung looks forward to meeting with President Clinton.

Mr Tung will also officiate at the opening ceremony of the new office premises of the Hong Kong Economic and Trade Office in Washington.

Mr Tung will be in Tokyo from October 15 to 17. He will call on ministers, parliamentarians and senior officials of the Japanese Government.

He will then leave for Europe on October 19 and visit Brussels and London before returning to Hong Kong on October 23.

- world problem. The program is designed for completion in one calendar year of full-time study.
5. Master of Entertainment Technology degree requires 177 units of course work and is jointly offered by CMU's College of Fine Arts and School of Computer Science. It is a full-time, two-year program.
  6. Master of Human-Computer Interaction program aims to prepare students to participate in the design and implementation of software systems that can be used easily, effectively and enjoyably. The program supports membership from the School of Computer Science, the Graduate School of Industrial Administration, the School of Humanities and Social Sciences, the College of Fine Arts, the Robotics Institute, and the Software Engineering Institute, and a research and teaching faculty with a substantial focus on human use of computing. The program can be completed on a full-time basis in twelve months; two semesters and one summer. The curriculum consists of ten conventional semester-long courses and an extensive team-oriented studio/project experience. Students take courses, often at the advanced undergraduate level, to obtain a broad background in computer science, human behavior, design, and evaluation and assessment, and may elect to take more advanced courses to deepen their knowledge in a more specific area.
  7. Master of Science in Knowledge Discovery and Data Mining curriculum is based on core academic courses on Automated Learning and Discovery, Statistical Approaches for Learning and Discovery, and Algorithms for Learning and Discovery. Students also gain hands-on experience through Project Work, and a Lab Course. The third component of the curriculum consists of elective courses drawn from computer science, statistics and other relevant disciplines. The program can be completed via a 12-month course of full-time study during 3 consecutive Fall, Spring, and Summer terms, or via a 2-year (4 academic term) course of study, including project work during the intervening summer. This track is designed primarily for those intending to apply for a Research or Teaching Assistantship.
  8. Master of Science in Language Technologies (MLT) curriculum will consist of 120 or more course units, at least 96 of which must be selected from this list of MLT-approved core courses (most will be 12 units/course), which include the hands-on self-paced laboratory and the 24-unit Software Engineering for LT. These courses assume knowledge of programming and data structures. The curriculum is targeted primarily toward a professional degree; with some modifications and enhancements, it also forms the course-based component of the Ph.D. program. We expect some of the more research-oriented MLT students to apply for continuing studies into their Ph.D., with most of their MLT courses and hands-on work being credited towards the Ph.D.
  9. Master of Science in Robotics program is designed for completion by full-time students in 12 months. There are also a limited number of research and teaching assistantships available. An advanced degree in robotics requires both understanding a range of technical fields, and having experience with synthesizing real systems. The curriculum for the Master's degree reflects both the breadth and the hands-on nature of Robotics. The

(a) Binary front side image

(b) Grayscale back side image



(c) Synthetic show-through image

Figure 5. 10 Example of binary front side image

The more interesting case, where both front and back side images are grayscale, uses the following equation to compute the new bleed-through/show-through image:

$$g(\cdot) = \Phi(f(\cdot), H \otimes R(b(\cdot))) + N$$

where  $f(\cdot)$  is the front side image,  $b(\cdot)$  is the back side image,  $R(\cdot)$  is the reverse function,  $H$  is the “blurring matrix” corresponding to a shift-invariant point-spread function,  $N$  is assumed here to be additive and independent identical noise,  $g(\cdot)$  is the generated bleed-through/show-through image,  $\Phi(\cdot, \cdot)$  is the transformation function. In our preliminary experiments, we choose  $\Phi(\cdot, \cdot)$  as a linear function to simplify the model. If the front side image and back side image are not the same size, we resize the back side image to the size of front side image in the preprocessing stage. Then for each pixel  $(i, j)$

$$\Phi_{i,j}(f_{i,j}, B_{i,j}) = \begin{cases} f_{i,j} - \alpha(f_{i,j} - B_{i,j}) + \eta_{i,j} & \text{if } f_{i,j} - B_{i,j} > \text{ithreshold} \\ f_{i,j} + \eta_{i,j} & \end{cases}$$

where:

$B$ :  $H \otimes R(b(\cdot))$ , i.e. blurred and reversed back side image

$\alpha$  and  $\text{ithreshold}$ : parameters to control the attenuation rate.

This model is based on two observations. The first is that only when the intensity difference between front and back side image is large enough, there is show-through effect. In other words, if the front side pixel is too dark, or the back side pixel is too light, the intensity of the original front side pixel becomes dominant in the new pixel. The second observation is that show-through can only make the new pixel

darker than front side pixel. To justify our method, an example is given in the following section.

### **5.4.3 Experiments**

We generated a synthetic image from the proposed approach, and compare it visually with the real scanned newspaper image, such as Figure 5.9 to demonstrate the effectiveness. Our goal was to obtain two blank newspaper pages with same size and quality, print some text on the first sheet, and scan it to obtain the front side image. Then obtain the back side image using the same method with the second sheet. Finally print the back side image on the back side of the first sheet to obtain the real scanned image with show-through effect. Because it is hard to obtain the machine similar to those printing newspapers and blank newspaper, we extracted the front side image and back side image directly from Figure 5.9.

To obtain a “pure” back side image of the newspaper, we place a black paper between the newspaper and scanner backing to limit undesirable scan-through effect, not remove it completely. However, it is acceptable due to the fact that the intensity of back side pixel attenuates significantly in generating the show-through image, and the faint show-through effect on back side image decays much faster. It is hard to obtain a “pure” front side image in this way because the intensity of front side pixels are usually dominant in generating scan-through image, which is thus sensitive to the “seeping” ink.

Fortunately, we can separate the scanned image into three layers: foreground, which is the printed text or figures; background, which contains mostly the texture of newspaper; and the unwanted reverse side layer. With the thresholds calculated

through the newspaper image, we cluster the pixels into three layers, and remove those labeled as unwanted layer. To make the background smoother, we use the nearest background pixel intensity to fill in the positions of removed pixels. Figure 5.11 shows the front side image and back side image respectively. There is almost no show-through effect in the front side image now.

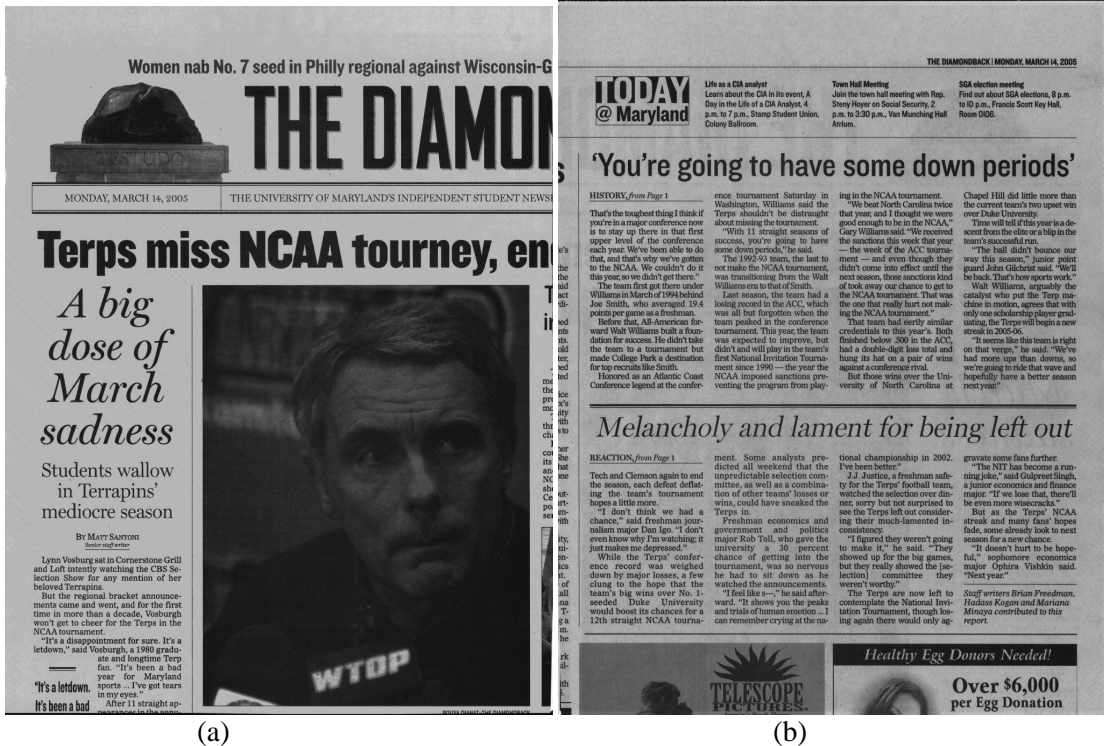


Figure 5.11 (a) Front side image; (b) Back side image from Figure 5.9

Figure 5.12 is the comparison of synthetically generated image and the real scanned image. Visually, they are similar. Because we have “filtered” some of the noise and stains when obtaining front side image, the synthetic image seems a little lighter and has a more homogeneous background. Thus improvement is possible if we can obtain the exact front side image. The parameter  $\alpha$  and threshold are currently chosen manually, but can be computed by analyzing the changes of the front side and back side image pixels.

Women nab No. 7 seed in Philly regional against Wisconsin-G



# THE DIAMOND

MONDAY, MARCH 14, 2005

THE UNIVERSITY OF MARYLAND'S INDEPENDENT STUDENT NEWS

## Terps miss NCAA tourney, end

### *A big dose of March sadness*

#### Students wallow in Terrapins' mediocre season

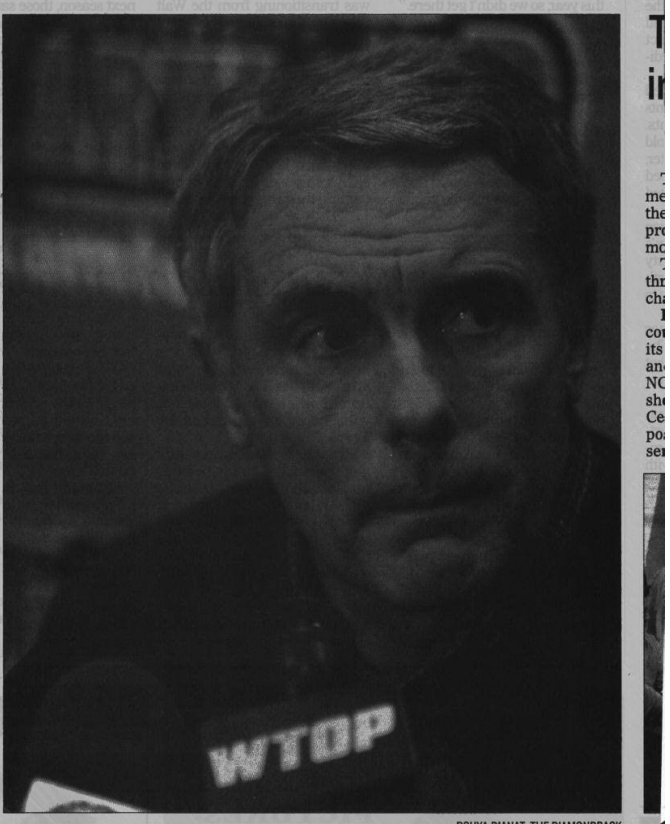
By MATT SANTONI  
*Senior staff writer*

Lynn Vosburg sat in Cornerstone Grill and Loft intently watching the CBS Selection Show for any mention of her beloved Terrapins.

But the regional bracket announcements came and went, and for the first time in more than a decade, Vosburgh won't get to cheer for the Terps in the NCAA tournament.

"It's a disappointment for sure. It's a letdown," said Vosburgh, a 1980 graduate and longtime Terp fan. "It's been a bad year for Maryland sports ... I've got tears in my eyes."

After 11 straight appearances in the annu



T  
in  
me  
the  
pr  
mc  
th  
ch  
I  
co  
its  
an  
NC  
sh  
Ce  
po  
se

(a)



(b)

Figure 5.12 (a) synthetically generated scan-through image with  $\alpha = 0.1$ , and threshold = 60  
 (b) real scanned newspaper

### 5.5 Implementation

All the degradation methods have been implemented in C++, and encapsulated into DLDegradation class, which can be incorporated and used as an

API in other systems. DLDegradation class uses the basic image data format defined in DocLib library. The following table is the functions and parameter list:

Noise Type	Parameters	Type	Min	Max
Blur	Filter Size	Int	3	11
	Std Deviation	Float	0	10.0
	Passes Number	Int	1	10
	Blur Probability	Float	0	1.0
	Threshold	Int	0	255
Resolution	Horizontal Res.	Int	50	Image Res.
	Vertical Res.	Int	50	Image Res.
	Threshold	Folat	0.0	100.0
HLINE	Min. Length	Int	1	Image width - 1
	Max. Length	Int	Min. Length	Image width
	Min. Width	Int	1 (-1) <sup>1</sup>	20 (-20) <sup>1</sup>
	Max. Width	Int	Min. Width	20 (-20) <sup>1</sup>
	Min. Density	Float	0.0	1.0
	Max. Density	Float	Min. Density	1.0
	Number of Lines	Int	1	100
VLINe	Min. Length	Int	1	Image height - 1
	Max. Length	Int	Min. Length	Image height
	Min. Width	Int	1 (-1) <sup>1</sup>	20 (-20) <sup>1</sup>
	Max. Width	Int	Min. Width	20 (-20) <sup>1</sup>
	Min. Density	Float	0.0	1.0
	Max. Density	Float	Min. Density	1.0
	Number of Lines	Int	1	100
Rotation	Rotate Point X	Int	N/A	N/A
	Rotate Point Y	Int	N/A	N/A
	Rotate Angle	Float	-180.0	180.0
Speckles	Dist. Values for 10 Sizes	Float	0.0	100.0
	Probability	Float	0.0	1.0
Pixelflip <sup>[5]</sup>	R.V. Seed	Int	0	N/A
	P <sub>0</sub>	Float	0.0	1.0
	A <sub>0</sub>	Float		
	B <sub>0</sub>	Float		
	A <sub>1</sub>	Float		
	B <sub>0</sub>	Float		
	D	Int	2	
Merge	Image file	string		
	Image file	String		
Show-through	$\alpha$	Float	0.0	1.0
	Threshold	Int	1	255

Table 4 Function and parameter list for document degradation class

Remark: 1. When specified as the negative, this function will remove lines from the image.

## Chapter 6 Summary

Ground truth collection plays an important role in document analysis system training and evaluation. Manually generating data sets is labor-intensive, and error-prone. Furthermore, it is prohibitively expensive to get representative multilingual data sets with thousands of pages. Using existing data sets may partly alleviate the cost. However, it is not flexible enough to evaluate the underlying system, which may require specific vocabulary and special document styles. With the increased interest in processing multilingual sources, however, there is a tremendous need to be able to rapidly generate data in new languages and scripts, without the need to develop specialized systems.

### 6.1 Summary of contributions

The main contributions presented in this thesis are:

1. We have proposed and implemented a methodology to automatically generate ground truth from electronic text. This method produces the complete ground truth, including symbolic text files and noise free images at different resolutions, which can be used in training or evaluating document analysis systems. It is extremely flexible and convenient when dealing with new languages and scripts. For most of the languages of interest, the electronic text can be copied and pasted from the website so that no manual input processing is needed.

2. We have proposed a method to transform ground truth files from ideal images to degraded images. This method modeled the transformation as a linear projective transformation. Because we use four feature points to position the bounding boxes of document, our method is robust in noisy documents.
3. We have integrated a multi-lingual OCR evaluation system, and have evaluated two Chinese OCR systems.
4. We have proposed and implemented a document image degradation methodology. This method incorporates page level and pixel level noise often encountered in printing, copying, faxing, and scanning. Rotation, blur, scattering lines, resolutions change, noise template merge, speckles, jitter, pixel drift, and show-through are included in this method.

## Reference

- [1] D. Doermann, and S. Yao, "Generating Synthetic Data for Text Analysis Systems", *Symposium on Document Analysis and Information Retrieval*, pp. 449-467, 1995
- [2] Y. Li, D. Lopresti, G. Nagy, and A. Tomkins, "Validation of Image Defect Models Optical Character Recognition", *IEEE Transactions on Pattern Analysis and Machine Intelligence*, vol. 18, no. 2, pp. 99-108, 1996
- [3] H.S. Baird, "The State of the Art of Document Image Degradation Modeling", In *Proc. of 4th IAPR International Workshop on Document Analysis Systems*, Rio de Janeiro, Brazil, pp.1-16, 2000
- [4] R.M. Haralick, I. Phillips, et al., "UW CD-ROM"
- [5] T. Kanungo, "Document Degradation Models and a Methodology for Degradation Model Validation", Ph.D. Dissertation, University of Washington, Seattle, 1996. <http://www.cfar.umd.edu/~kanungo/pubs/publications.html>
- [6] T. Kanungo and P. Resnik, "The Bible, Truth, and Multilingual OCR Evaluation", *TR: LAMP-TR-029/CFAR-TR-902/CS-TR-3967*, University of Maryland, College Park, Dec. 1998
- [7] George Nagy, "Twenty Years of Document Image Analysis in PAMI", *IEEE Transactions on Pattern Analysis and Machine Intelligence*, vol. 22, no. 1, pp. 38-62, 2000
- [8] T. Kanungo and R. M. Haralick, "An Automatic Closed-Loop Methodology for Generating Character Groundtruth for Scanned Documents," *IEEE Transactions on Pattern Analysis and Machine Intelligence* vol. 21, no. 2, pp. 179-183, February, 1999
- [9] D.W. Kim and T. Kanungo, "Attributed Point Matching for Automatic Groundtruth Generation", *Int'l Journal on Document Analysis and Recognition*, vol. 5, no. 1, pp. 47-66, 2002
- [10] Greg Arzoomanian and Richard Weeks, GroundsKeeper, <http://documents.cfar.umd.edu/resources/source/ppanther/gkpr.html>
- [11] T. Kanungo, C. Lee, J. Czorapinski and I. Bella, "TRUEVIZ: A groundTRUth/metadata Editing and VISualiZing Toolkit for OCR," *SPIE Conference on Document Recognition and Retrieval VIII*, Vol. 4307, San Jose CA, January 2001

- [12] V. Märgner and M. Pechwitz, "Synthetic Data for Arabic OCR System Development", *Proc. Of Int'l Conference on Document Analysis and Recognition*, pp. 1159-1163, Seattle, Washington, Sep. 2001
- [13] T. Varga and H. Bunke, "Generation of Synthetic Training Data for an HMM-based Handwriting Recognition System", *Proc. Of Int'l Conference on Document Analysis and Recognition*, pp618-622, 2003
- [14] J. Zhai, W. Liu etc, "A line drawing degradation model for performance characterization", *Proc. Of Int'l Conference on Document Analysis and Recognition*, pp618-622, 2003
- [15] H.S. Baird, "Document Image Defect Models", in H.S. Baird, H. Bunke, and K. Yamamoto, editors, *Structured Document Image Analysis*, pp. 546-556, Springer-Verlag, NY, 1992
- [16] H.S. Baird, "Document Image Quality: Making Fine Discriminations", *Proc. Of Int'l Conference on Document Analysis and Recognition*, pp. 20-22, Bangalor, India, Sep. 1999
- [17] T.K. Ho, Henry S. Baird, "Evaluation of OCR Accuracy Using Synthetic Data", *Symposium on Document Analysis and Information Retrieval*, pp. 413-422, 1995
- [18] T. Kanungo, R.M. Haralick, and I.T. Phillips, "Nonlinear local and global document degradation models", *Int'l J. Imaging System and Technology*, vol. 5, no. 4, pp. 220-230, 1994
- [19] A. Zramdini and R. Ingold, "A Study of Document Image Degradation Effects on Font Recognition", *Proc. Of Int'l Conference on Document Analysis and Recognition*, pp740~743, 1995
- [20] P. Sarkar, H. S. Baird, and X. Zhang, "Training on severely degraded text-line images," *Proc. Of Int'l Conference on Document Analysis and Recognition*, pp. 38-43, 2003
- [21] I. T. Phillips, "How to extend and bootstrap an existing data set with real-life degraded images", *Proc. Of Int'l Conference on Document Analysis and Recognition*, pp: 689-692, 1999
- [22] S. Sural And P.K. Das, "A two-state Markov chain model of degraded document images," In *Proc. Of Int'l Conference on Document Analysis and Recognition*, pp. 463-466, Bangalor, India, Sep. 1999
- [23] T. Kanungo, G.E. Marton, and O. Bulbul, "Performance Evaluation of Two Arabic OCR Products," *Proc. of AIPR Workshop on Advances in Computer Assisted Recognition*, SPIE vol. 3584, Washington DC, October, 1998

- [24] S. Chen, S. Subramaniam, I. T. Phillips, and R. M. Haralick, "Performance evaluation of two OCR systems," in *Proc. Symposium on Document Analysis and Information Retrieval*, April 1994, pp. 299-317
- [25] Feng Yuan, "Windows Graphics Programming: Win32 GDI and DirectDraw", Prentice Hall PTR, Upper Saddle River, 2001
- [26] <http://www.unicode.org>
- [27] "TrueType specifications",  
<https://www.microsoft.com/typography/specs/default.htm>
- [28] Esko Ukkonen, "Algorithm for Approximate String Matching", *Information and Control* vol. 64, pp. 100-108, 1985
- [29] S.V. Rice, F.R. Jenkins, and T.A. Nartker, "The fifth annual test of OCR accuracy," Tech. Rep. TR-96-01, Information Science Research Institute, University of Nevada, Las Vegas, NV, 1996
- [30] T. Kanungo, G. A. Marton, O. Bulbul, "OmniPage vs. Sakhr: Paired Model Evaluation of Two Arabic OCR Products," *Proc. of SPIE Conference on Document Recognition and Retrieval (VI)*, vol. 3651, San Jose, CA, 1999
- [31] A. Tonazzini, L. Bedini, E. Salerno, "Independent component analysis for document restoration", *International Journal on Document Analysis and Recognition*, vol. 7, pp. 17-27, 2004
- [32] G. Sharma, "Show-Through Cancellation in Scans of Duplex Printed Documents", *IEEE Transactions on Image Processing*, vol. 10, no. 5, pp. 736-754, May 2001
- [33] S. Geman and D. Geman, "Stochastic relaxation, Gibbs distributions and Bayesian restoration of images," *IEEE Trans. Pattern Anal. Machine Intell.*, vol 6, 721-741, 1984
- [34] Gang Zi, David S. Doermann, "Document Image Ground Truth Generation from Electronic Text," *ICPR*, (2), pp: 663-666, UK, 2004
- [35] D. Doermann and G. Zi, "Groundtruth Image Generation from Electronic Text (Demonstration)," *Symposium on Document Image Understanding Technology*, pages 309-312, April 2003